AD_____

Award Number: DAMD17-01-1-0178

TITLE: Anti-Angiogenic Therapeutic Indicators in Breast Cancer

PRINCIPAL INVESTIGATOR: Min-Ying L. Su, Ph.D.

CONTRACTING ORGANIZATION: University of California
Irvine, California 92697-1875

REPORT DATE: August 2003

TYPE OF REPORT: Annual

PREPARED FOR: U.S. Army Medical Research and Materiel Command
Fort Detrick, Maryland 21702-5012

DISTRIBUTION STATEMENT: Approved for Public Release;
Distribution Unlimited

The views, opinions and/or findings contained in this report are
those of the author(s) and should not be construed as an official
Department of the Army position, policy or decision unless so
designated by other documentation.

20040329 047

REPORT DOCUMENTATION PAGE

Form Approved
OMB No. 074-0188

1. AGENCY USE ONLY (Leave blank)	2. REPORT DATE August 2003	3. REPORT TYPE AND DATES COVERED Annual (2 Jul 2002 – 1 Jul 2003)

4. TITLE AND SUBTITLE
Anti-Angiogenic Therapeutic Indicators in Breast Cancer

5. FUNDING NUMBERS
DAMD17-01-1-0178

6. AUTHOR(S)
Min-Ying L. Su, Ph.D.

7. PERFORMING ORGANIZATION NAME(S) AND ADDRESS(ES)
University of California, Irvine
Irvine, California 92697-1875

E-Mail: msu@uci.edu

8. PERFORMING ORGANIZATION REPORT NUMBER

9. SPONSORING / MONITORING AGENCY NAME(S) AND ADDRESS(ES)
U.S. Army Medical Research and Materiel Command
Fort Detrick, Maryland 21702-5012

10. SPONSORING / MONITORING AGENCY REPORT NUMBER

11. SUPPLEMENTARY NOTES
Original contains color plates: All DTIC reproductions will be in black and white.

12a. DISTRIBUTION / AVAILABILITY STATEMENT
Approved for Public Release; Distribution Unlimited

12b. DISTRIBUTION CODE

13. ABSTRACT (Maximum 200 Words)
This project studies the therapeutic indicators in ant-angiogenic therapy. Every animal with mammary tumor was scheduled to receive a baseline MRI, core biopsy, then followed by 4 treatments with weekly MRI follow-up. The tumors were categorized into responders, stabilizers, and non-responders depending on the final tumor size compared to the baseline size. The results obtained so far indicated that majority of infiltrating adenocarcinomas were responders and all papillary adenocarcinomas were responders and all papillary adenocarcinomas were stabilizer. The relationship between response and tumor type will be fully investigated when all data are available. In the responders, the Gd-DTPA-BMA enhancement at 2-min after injection showed a decreasing trend with treatment, which was not observed in the non-responders. However, the changes of MRI enhancement parameters with treatment did not show a significant differences among different response groups. We also completed the immunohistochemical staining study using available specimens of ENU induced tumors from another project. The ductal adenocarcinoa had the highest microvessel density, then in order were papillary adenocarcinoma, fibroadenoma, and the adenosis had the lowest microvessel density, which was consistent with the degree of malignancy and benignity. The IHC study on the tumors undergoing chemotherapy are currently in progress.

14. SUBJECT TERMS
Breast Cancer

15. NUMBER OF PAGES
28

16. PRICE CODE

17. SECURITY CLASSIFICATION OF REPORT	18. SECURITY CLASSIFICATION OF THIS PAGE	19. SECURITY CLASSIFICATION OF ABSTRACT	20. LIMITATION OF ABSTRACT
Unclassified	Unclassified	Unclassified	Unlimited

Table of Contents

(4)   Introduction

Anti-angiogenic therapy is a promising alternative for treatment of cancer, also it may be used as maintenance therapy to prevent metastasis or recurrence. While 60% of the approximately 186,000 annual cases of breast cancer now present as node negative, 30% of these cases will recur after local therapy. Although adjuvant chemotherapy has been demonstrated to improve survival in node negative breast cancer, it is still unclear how best to identify those patients whose risk of metastatic disease exceeds their risk of significant therapeutic toxicity. On the other hand, for treatment of locally advanced disease, anticancer chemotherapy has produced only modest gains. Newer therapeutic strategies are greatly needed. Anti-angiogenic therapy maybe used to augment the efficacy of the traditional cytotoxic therapeutic agents. Furthermore, a new line of therapy that has a less side toxicity effect is definitely needed to provide the patients with more options for treatment. Because angiogenesis appears to play an important role in the disease progression, anti-angiogenic agents may have a great potential for treating breast cancer.

While the efficacy of traditional therapeutics has been determined by measuring tumor response and patient survival, these newer approaches may prolong life and improve symptoms by stabilizing tumor progression rather than by causing tumor shrinkage. It is therefore necessary to develop improved endpoints that can determine the clinical activity of these agents during their development. In this project we used in vitro and in vivo strategies to measure the potential efficacy of anti-angiogenic compounds in order to facilitate their clinical development. Two breast cancer models, R3230 AC adenocarcinoma and carcinogen N-ethyl-N-nitrosourea(ENU) induced mammary tumors will be used, and two drugs known to have anti-angiogenesis effect, taxotere and thalidomide, will be used to treat cancers. We will measure the therapy induced changes using the in vivo magnetic resonance imaging and the in vitro immunohistochemistry. Dynamic contrast enhanced MRI has been shown as a non-invasive means to measure the vascular characteristics in tumors. We will apply this technique to measure the longitudinal structural and vascular changes taking place in tumors following treatment. While these structural and vascular changes observed by MRI are macroscopic, they are governed by the underlying biological changes, e.g. the decrease of microvessel density and changes of other angiogenic markers. The vascular changes measured by MRI will be correlated with the neovessel density count (obtained by immunohistochemistry with CD105 staining) and the angiogenesis index (AI, constituting 3 angiogenic markers, p53, TSP-1, CD31) and expression level of VEGF.

After completion of this pilot study we expect to achieve three goals: (1) to assess the feasibility of using these two animal models for testing the efficacy of other potential anti-angiogenic compounds, (2) to identify other therapeutic indicators rather than tumor shrinkage (immunohistochemical markers or MRI cellular and vascular parameters) for determination of therapeutic efficacy, (3) to find early therapeutic indicators which will predict the final outcome.

(5) Body

Five specific aims were proposed. First we will establish the tumor models. For each tumor, when the size reaches 1.0 cm the baseline MRI study will be performed. After the MRI study core needle biopsy will be performed to obtain tissue specimens for analysis of baseline angiogenic biomarkers. Then the tumor will receive treatment. Several MRI studies will be performed to follow the longitudinal changes. At the conclusion of the study the animal will be sacrificed, and the tumor excised for measures of post-treatment angiogenic biomarkers.

Aim 1.   Establish the R3230 AC adenocarcinoma and ENU induced mammary tumor models.

Aim 2.   Perform the baseline dynamic contrast enhanced MRI before administration of therapeutic drugs to measure the pre-treatment characteristics of tumors.

Aim 3.   Perform core needle biopsy to obtain cancer specimens for evaluation of baseline angiogenic activity using immunohistochemical analysis.

Aim 4.   Apply dynamic contrast enhanced MRI to monitor the longitudinal volumetric, cellular and vascular changes taking place in tumors following therapy.

Aim 5.   Perform immunohistochemical studies to measure the CD105 neovessel density, VEGF, and the angiogenesis index (AI) markers in tumors for assessment of anti-angiogenic effects.

At beginning of this project in Yr-01, 53 rats were injected with carcinogen ENU, and to date 46 mammary tumors were found. Among these 46 tumors, 29 tumors completed all MRI studies, including the baseline and 3 follow-up. The response was determined, and the contrast enhancement parameters were obtained for each tumor. During last year immunohistochemical studies were performed on the ENU tumor specimens obtained from another study. The results are summarized below. The tumor biopsy and the whole tumor specimens obtained from this study are currently being analyzed with immunohistochemical staining. Therefore Aim 5 has not been completed yet. No-cost extension has been filed to complete all immunohistochemical studies and statistical analysis. When all data are available, they will be included in the final report.

ENU induced tumors undergoing chemotherapy

Introduction: Anticancer chemotherapy has produced only modest gains in the treatment of solid tumors. Newer therapeutic strategies are greatly needed. Anti-angiogenic therapy is one of the most promising novel approaches. While the efficacy of traditional therapeutics has been determined by measuring tumor response, these newer approaches may prolong life and improve symptoms by stabilizing tumor progression rather than by causing tumor shrinkage. It is therefore necessary to develop improved endpoints that can determine the clinical activity of these agents. In this study we

investigated whether the vascular parameters measured by dynamic contrast enhanced MRI can differentiate responder vs. non-responders in tumors receiving Toxotere as treatment.

Methods: 53 Sprague-Dawley rats were injected with 90 mg/kg carcinogen ENU (N-ethyl-N-nitrosourea). The tumor started to appear 2 moths after the injection. The baseline MRI was conducted when the tumor reached 0.7 cm in diameter. The imaging protocol included a T2-weighted sequence for volumetric measurement, and the dynamic study using a small molecular weight agent Gd-DTPA-BMA (®Omniscan, 0.1 mmol/kg), followed by an intermediate molecular weight agent Gadomer-17 (0.05 mmol/kg). After the MRI study was completed the rats received i.v. injection of 4 mg/kg Toxotere. Three follow-up MRI studies were performed, once per week. The rats continued to receive weekly Toxotere treatment after each MRI study.

Results: Forty-six mammary tumors have been found to date. Other non-mammary tumors (most often sarcoma and renal carcinoma) were also found but not studied. Among these 42 tumors, 29 tumors have completed the longitudinal study at 4 time points (noted as baseline study, and follow-up studies at week-1, week-2, and week-3). According to the tumor volume at the end of week-3 compared to the baseline (noted as GR), the tumor was classified into responder ($GR < 0.5$), stabilizer ($0.5 < GR < 1.5$), and non-responder ($GR > 1.5$). Figure 1 shows the growth curves of all tumors in each group. Some variations were noted in each group, but the general trend was distinctly different among the 3 groups.
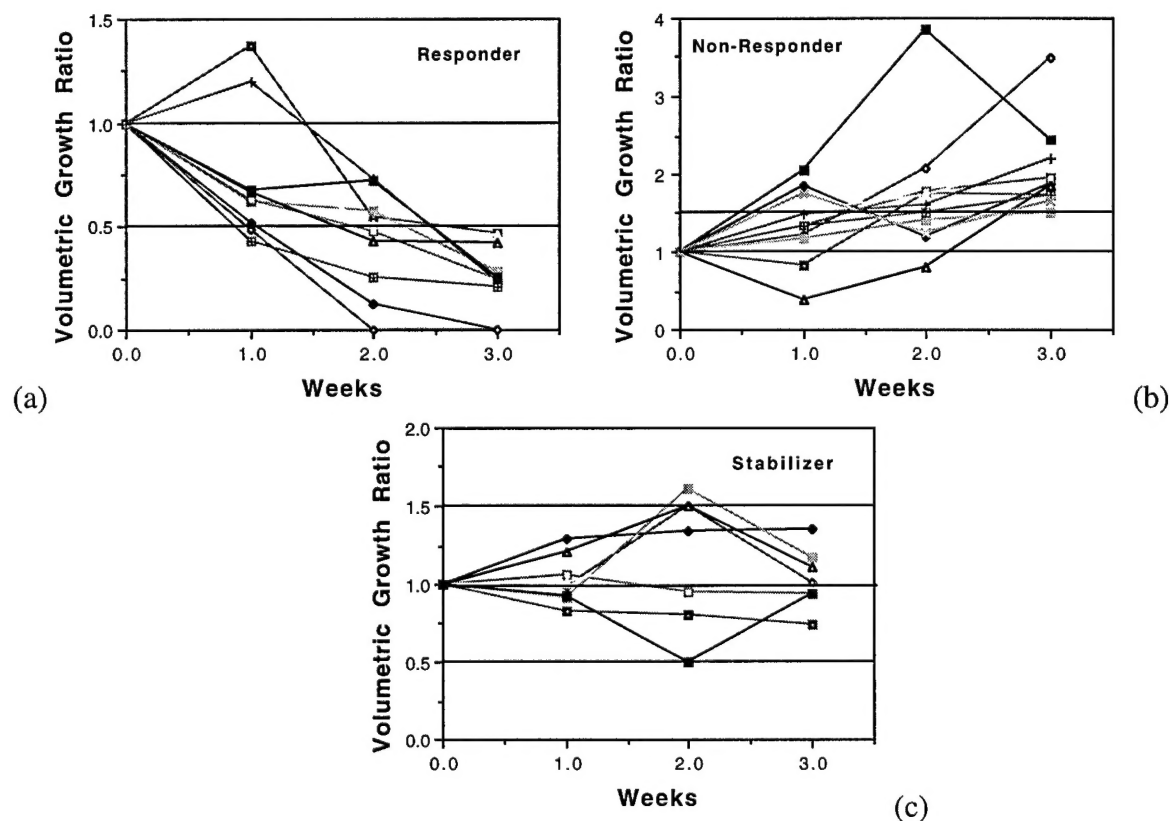

(a)

(b)

(c)

Figure 1: The tumor volume at baseline (week-0) and 3 follow-up studies (weeks 1-3). According to the tumor volume at the end of week-3 compared to the baseline (noted as GR), the tumor was classified into responder (a, GR < 0.5), non-responder (b, GR > 1.5), and stabilizer (c, 0.5 < GR <1.5).

The T2-weighted images (from a center slice) of one tumor in each response group, as well as the enhancement kinetics measured by Gd-DTPA-BMA (®Omniscan) and Gadomer-17 are shown in Figures 2-4. The responder (an infiltrating adenocarcinoma) illustrated in Fig.2 showed a steady regression. In the Gd-DTPA-BMA enhancement kinetics, a substantial decrease was noted in week-1 compared to the baseline, also the pattern became more flattened (no clear wash-out as in the baseline). Gadomer-17 showed similar results. In the stabilizer (a papillary adenocarcinoma) illustrated in Fig.3, apparently the tumor size remained unchanged during the 3 weeks period. In the enhancement kinetics measured by both contrast agents, although the intensity magnitude varied, the patterns remained unchanged. The non-responder illustrated in Fig.4 was an infiltrating adenocarcinoma. The tumor grew larger and larger with time. In the enhancement kinetics, the patterns remained unchanged. The magnitude of Gadomer-17 enhancement reduced substantially at week-1 compared to the baseline, then increased at week-2 and again increased at week-3. Since the locations of the tumor were different in different animals, they might be placed at different regions of coil with non-uniform sensitivity, therefore the signal enhancement was normalized to the pre-contrast signal intensity, and the obtained % enhancement was used in the statistical analysis. The % enhancements at the 5th, 6th, and 10th time points were obtained from each tumor and compared among the three response groups.

Figure 2: The T2-weighted image(a), and the enhancement kinetics measured by Gd-DTPA-BMA(b) and Gadomer-17(c) in one responder tumor (infiltrating ductal adenocarcinoma). The tumor showed continuous regression over time. The kinetics measured by Gd-DTPA-BMA showed reduced intensity after the first treatment, and the pattern of the curve became more flattened (i.e. no wash-out).

Figure 3: The T2-weighted image(a), and the enhancement kinetics measured by Gd-DTPA-BMA(b) and Gadomer-17(c) in one stabilizer tumor (papillary adenocarcinoma) at baseline and week-1, week-2, week-3 follow up studies. The tumor sizes in the 4 studies were similar.
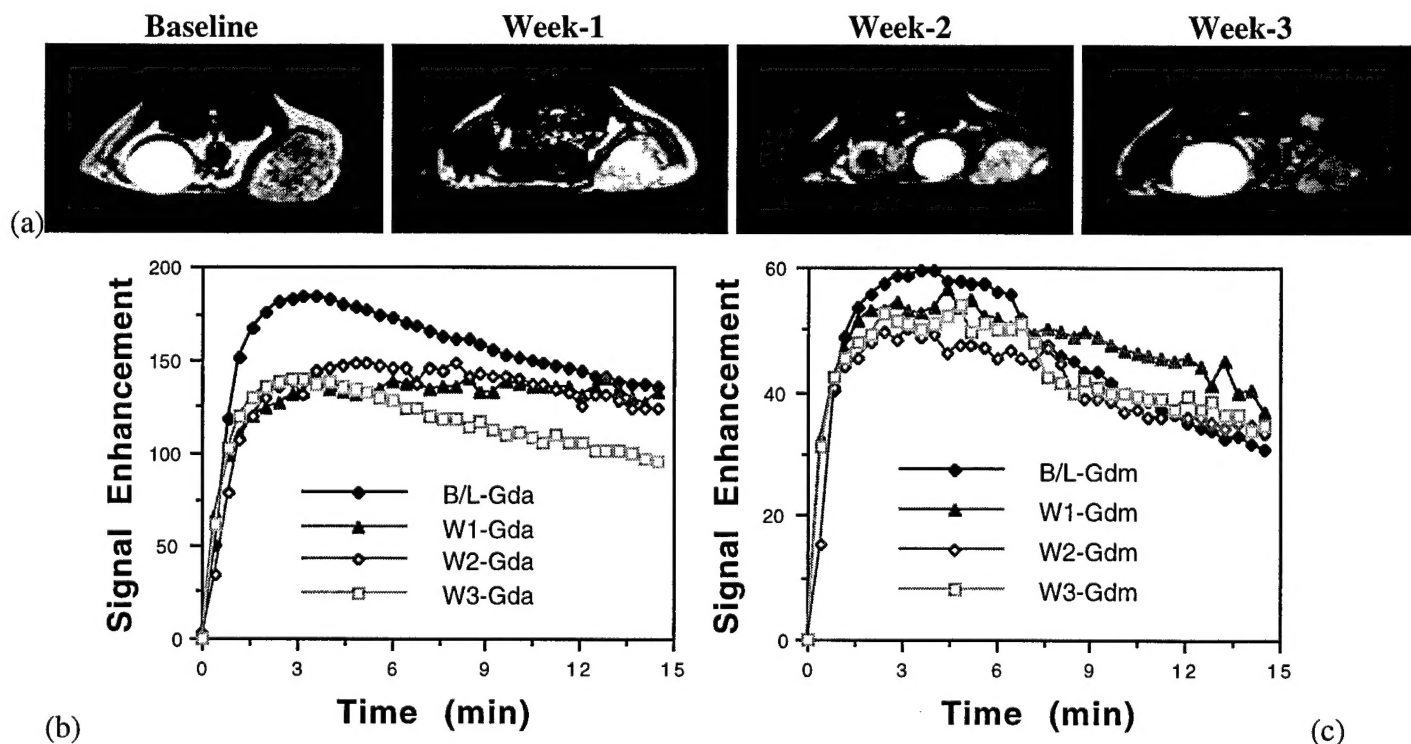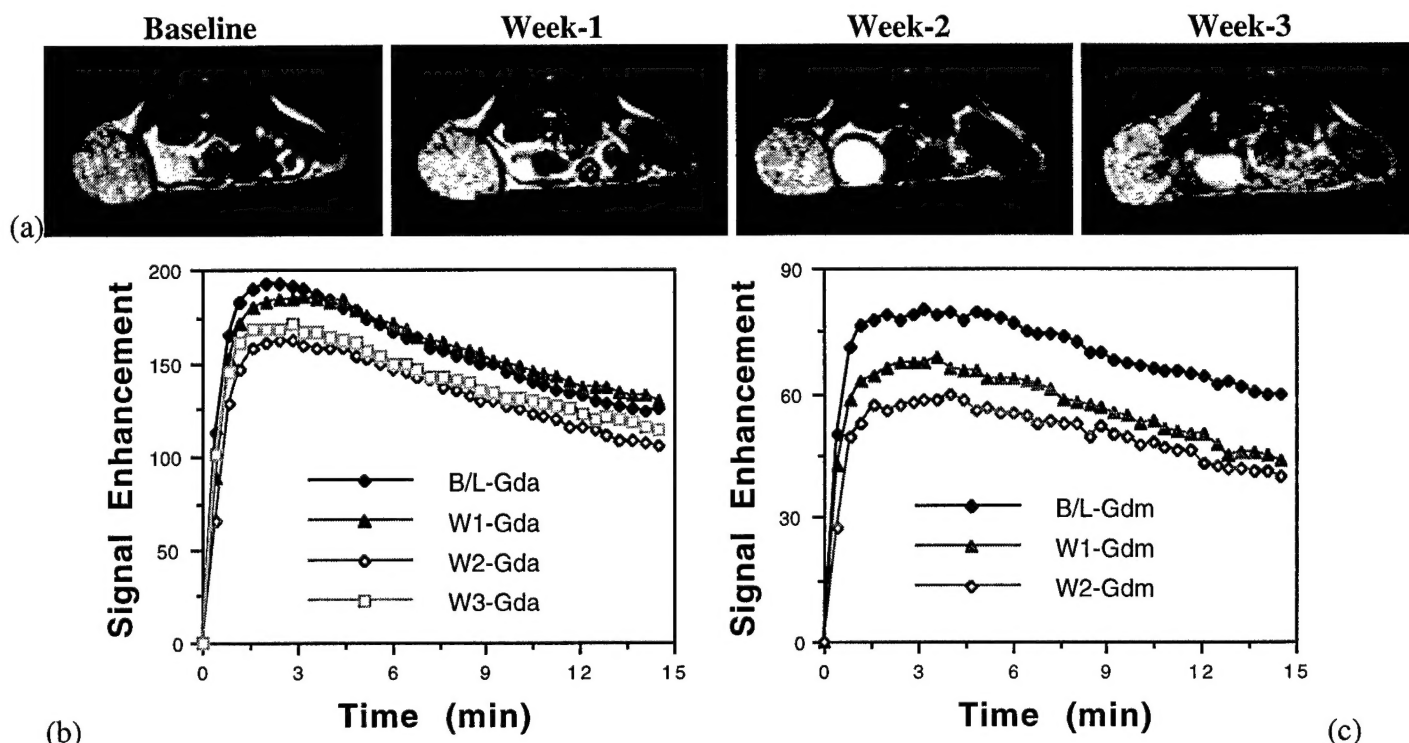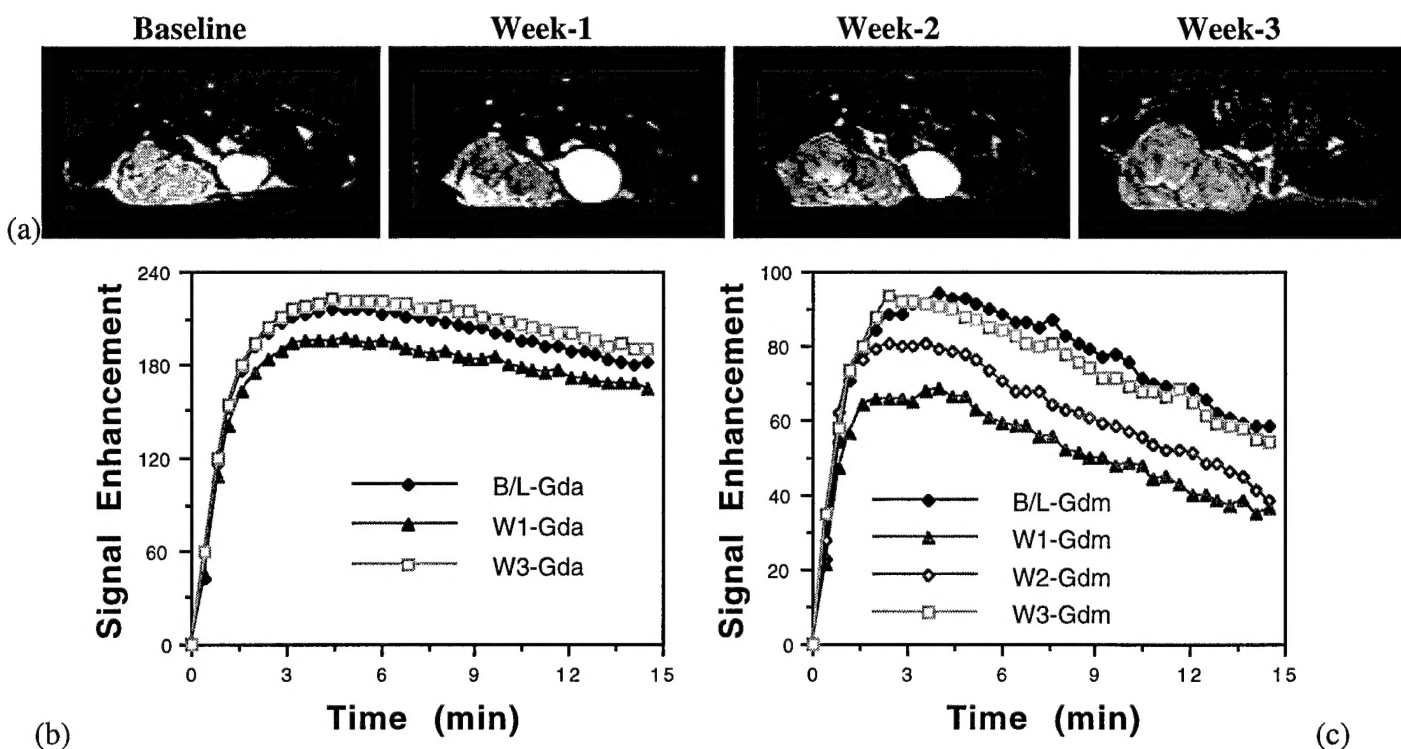
Figure 4: The T2-weighted image(a), and the enhancement kinetics measured by Gd-DTPA(b) and Gadomer-17(c) in one non-responder tumor (infiltrating ductal adenocarcinoma) at baseline and week-1, week-2, week-3 follow up studies. Apparently the tumor grew larger and larger over time.

The histological examination of all tumors are not completed yet. Only 19 tumors out of the 29 which had completed all MRI studies had confirmed diagnosis. Three tumor types were the most common, including infiltrating ductal adenocarcinoma (IDC), papillary adenocarcinoma (PAC), and the benign fibroadenoma (FA). Of these 19 tumors, 9 were responders (all were IDC), 5 were stabilizer (3 PAC and 2 IDC), and 5 were non-responders (4 IDC and 1 FA). Some IDC's were responders, some were stabilizer and some were non-responders. It would be interesting to find parameters which could serve as indicators to predict their responses. For each tumor the % enhancements at 5th, 6th, and 10th time points in the enhancement time course of Gd-DTPA-BMA and Gadomer-17 were measured. Figure 5 shows the mean and the standard deviation of all 14 IDC in the baseline and 3 follow-up studies. The Gd-DTPA-BMA % enhancement at the 10th time point showed a decreasing trend with treatment, but none of the parameters showed significant difference in the 4 studies (baseline and 3 follow-up). The 9 IDC responders and 4 IDC non-responders were analyzed separately, as shown in Figures 6 and 7. The decreasing trend was more clear in the subgroup of 9 responders. In contrast the 4 non-responders did not show any change at all. All 3 papillary adenocarcinomas diagnosed to date were stabilizers. These 3 tumors were analyzed as a subgroup, and the results are plotted in Figure 8. No changes were noted in this subgroup of PAC stabilizers either.
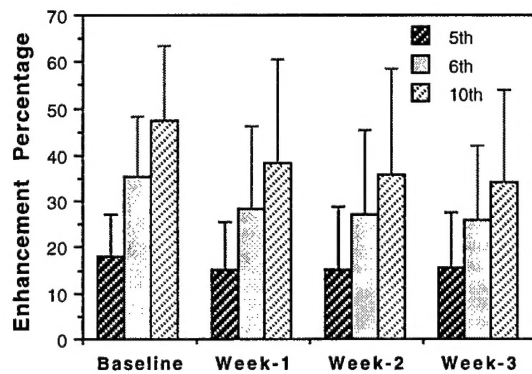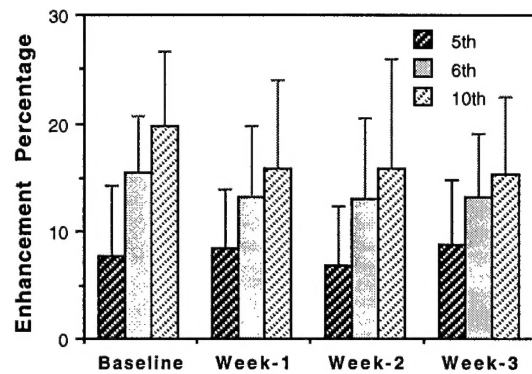
(a)   (b)

Figure 5: The mean and standard deviation of percent enhancement at 5th, 6th, and 10th time points (at 24 sec, 48 sec, and 2 min after injection) from al 14 IDC. The 10th Gd-DTPA-BMA percent enhancement showed a decreasing trend with treatment over time.

(a)   (b)

Figure 6: The mean and standard deviation of percent enhancement at 5th, 6th, and 10th time points, at 24 sec, 48 sec, and 2 min after injection of Gd-DTPA-BMA(a) and Gadomer-17(b), from the 9 IDC responders. The decreasing trend for the 10th Gd-DTPA-BMA percent enhancements was clear.

(a)   (b)

Figure 7: The mean and standard deviation of percent enhancement at 5th, 6th, and 10th time points, at 24 sec, 48 sec, and 2 min after injection of Gd-DTPA-BMA(a) and Gadomer-17(b), from the 4 IDC non-responders. The 10th Gd-DTPA-BMA percent enhancements did not show the decreasing trend as in the responder group in Figure 6.
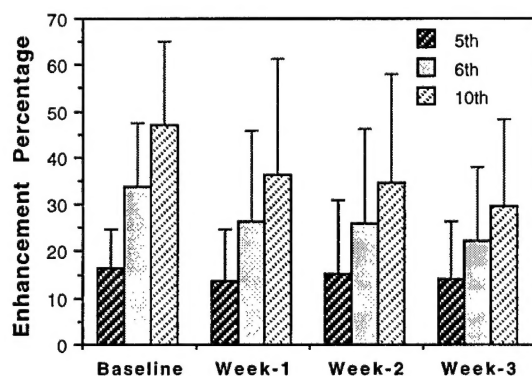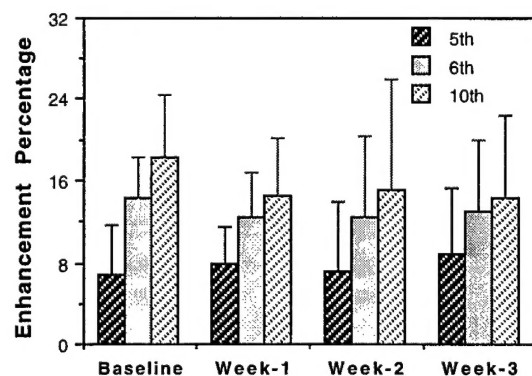
(a)

(b)

Figure 8: The mean and standard deviation of percent enhancement at 5th, 6th, and 10th time points, at 24 sec, 48 sec, and 2 min after injection of Gd-DTPA-BMA(a) and Gadomer-17(b) from the 3 PAC stabilizers. No substantial changes were noted.

In addition to the fibroadenoma in the non-responder group, 3 other FA's were found and the baseline studies were successfully completed. The baseline study of 3 other IDC's which did not complete all follow-up studies were also available. The baseline parameters for all 18 IDC, 4 FA, and 3 PAC were analyzed and shown in Figure 9. Consistent with previous findings, the fibroadenoma had slow enhancements at early time after injection of contrast agents, and the PAC had the highest enhancement magnitude.
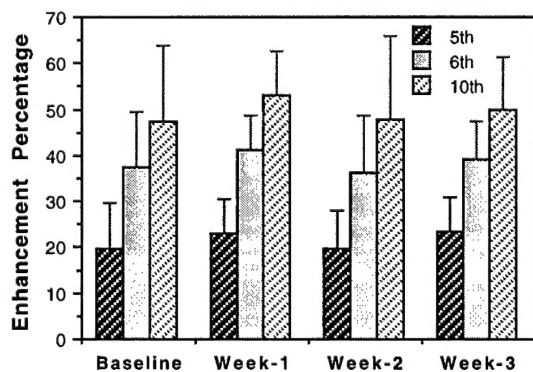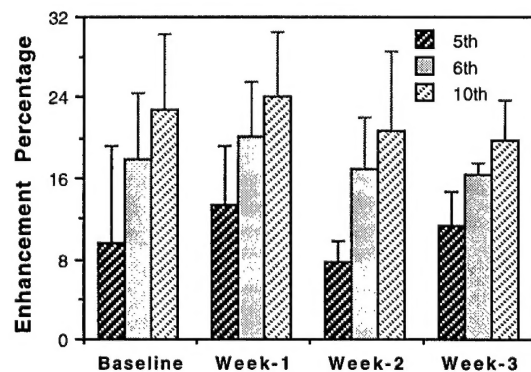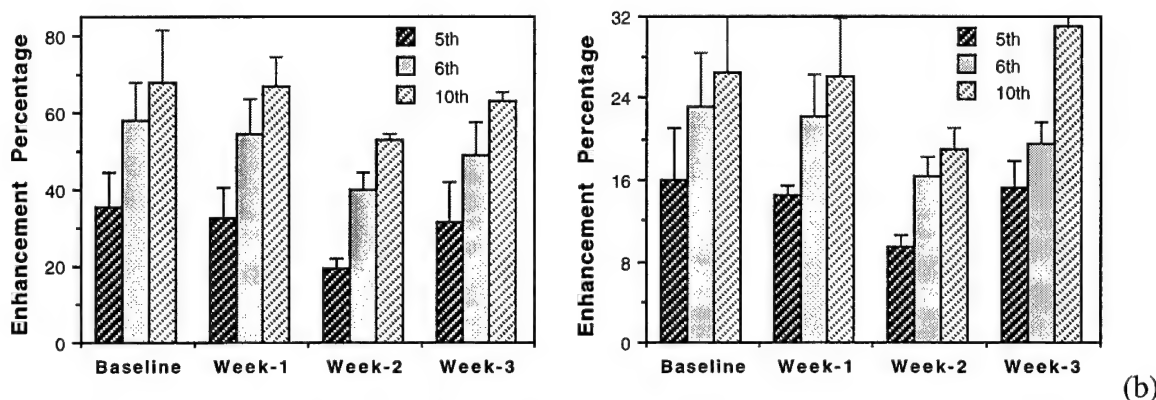

(a)

(b)
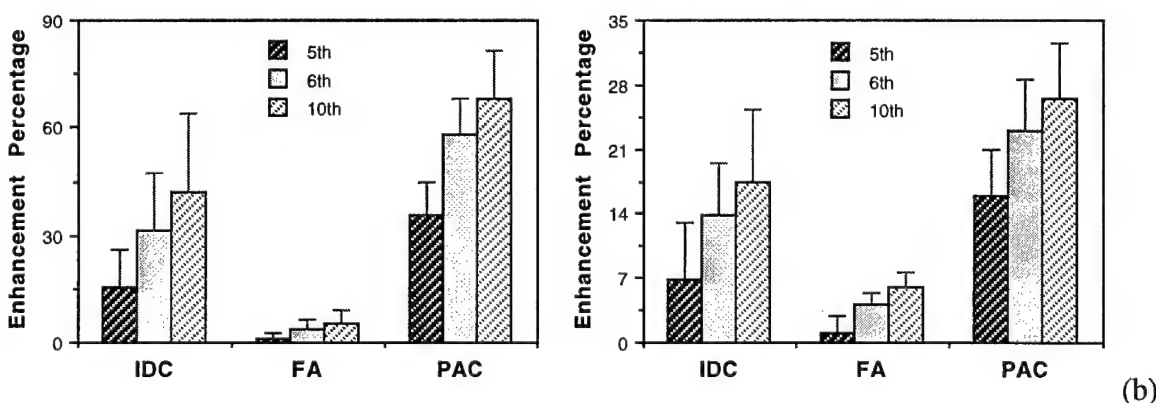
Figure 9: The mean and standard deviation of percent enhancement at 5th, 6th, and 10th time points, at 24 sec, 48 sec, and 2 min after injection of Gd-DTPA-BMA(a) and Gadomer-17(b) from all 18 IDC, 4 FA, and 3 PAC. PAC had the highest enhancements and the FA had the lowest enhancements at early times after injection.

In this experiment, all tumors received biopsy after the baseline MRI before receiving the first dose chemotherapy. After completing all follow-up MRI studies the animal was euthanized and the tumor was excised. If the animal died or had to be euthanized before completing all treatment and MRI studies, the tumor specimens were also obtained. These biopsy tissues and whole tumor specimens

page 11

were sent to Oncotech Inc. for immunohistochemical staining studies to measure the vessel density and expression of p53, TSP-1, and VEGF. The methods and some previous results will be summarized in the next section. The majority of IHC data from this chemotherapy study are not available yet, thus will be included in the final report.

Characterization of Angiogenesis in ENU Induced Benign And Malignant Mammary Tumors

Purpose

As the potential of anti-angiogenic or anti-vascular therapy for cancer treatment becomes more promising, the development of valid animal models as well as therapeutic efficacy markers have become increasingly important. The carcinogen ENU can induce benign and malignant tumors in rats, and the malignant tumors came with various SBR (Scarff-Bloom-Richardson) grades, thus it can be used as a suitable model for studies of angiogenesis. We applied dynamic contrast enhanced MRI and immunohistochemical (IHC) staining to study angiogenesis in the benign and malignant tumors of this model. Assessment of angiogenic biomarkers by immunohistochemical (IHC) staining is the most commonly used technique. For each specimen, we measured the expression level of mutant p53 (mp53), thrombospondin-1 (TSP-1), Vascular Endothelial Growth Factor (VEGF), and microvessel density (MVD) using Factor VIII staining. On the other hand, contrast enhanced imaging can be applied to measure the vascularity non-invasively. We utilized the broad spectrum of the ENU induced mammary tumor model and compared the angiogenesis measured using MRI and IHC molecular markers. Proper validation of imaging technique will facilitate its application in therapy monitoring, especially for anti-angiogenic or anti-vascular therapies.

Methods

N-ethyl-N-nitrosourea (ENU, 90 mg/kg) was injected i.p. into 30-day old SPF Sprague-Dawley rats (n=50) to induce mammary tumors. The tumors started to appear 2 months after injection. The baseline MRI study was performed when the tumor reached approximately 1.0 cm in diameter. For each tumor the enhancement kinetics of two contrast agents, the small agent Gd-DTPA-BMA (®Omniscan, 0.1 mmol/kg) and a mid-sized agent Gadomer-17 (0.05 mmol/kg, kindly provided by Schering AG, Germany), were measured. The volumetric growth rates, as well as the early (30-sec) and maximum (approximately 2-min) enhancements between benign and malignant tumors were compared. Each tumor was then surgically removed for IHC staining analysis to measure the expression of mp53, TSP-1, VEGF, and MVD. The rats were kept for observation of recurrence and further development of other tumors. The tumor types and angiogenesis of primary and subsequently developed tumors were compared.

Results

Ninety three tumors were found within 1 year after the injection of ENU. Most tumors belonged to four major types, 2 malignant and 2 benign. The malignant tumors included ductal adenocarcinoma (n=25) and papillary adenocarcinoma (n=21), and the two major benign lesions

were fibroadenoma (n=24) and adenosis (n=13). Multiple tumors (up to 5) could develop in one rat, all at different locations. No tumor recurrence was observed at the surgical site after removal of a previous tumor. The subsequently developed tumors were not associated with the primary tumor. In MRI studies, two malignant tumors exhibited similar enhancement kinetics, showing rapid early enhancing slope and high enhancement magnitude. Figure 10 shows the enhancement kinetics measured by Gd-DTPA-BMA (a) and Gadomer-17 (b) from these 4 tumors, one from each type. Two benign lesions had much slower early enhancing slope (highly significantly). The volumetric growth rates showed large variations even within each tumor type, and they were not correlated with the enhancement kinetics of both studied contrast agents. In IHC studies, the ductal adenocarcinoma had the highest microvessel density, then in order were papillary adenocarcinoma, fibroadenoma, and adenosis had the lowest microvessel density. All tumors had wild type p53. VEGF and TSP-1 were not significantly different among the 4 types. Higher vessel density was associated with higher MRI enhancement. Table 1 summarizes the growth rates, 30-sec and 2-min MR contrast enhancements and the IHC data.

Table 1: The growth rate, Gd-DTPA-BMA and Gadomer-17 enhancements at 30-sec and 2-min and the IHC biomarkers: factor VIII microvessel density, VEGF histo-score and TSP-1 optical density in 4 tumor types

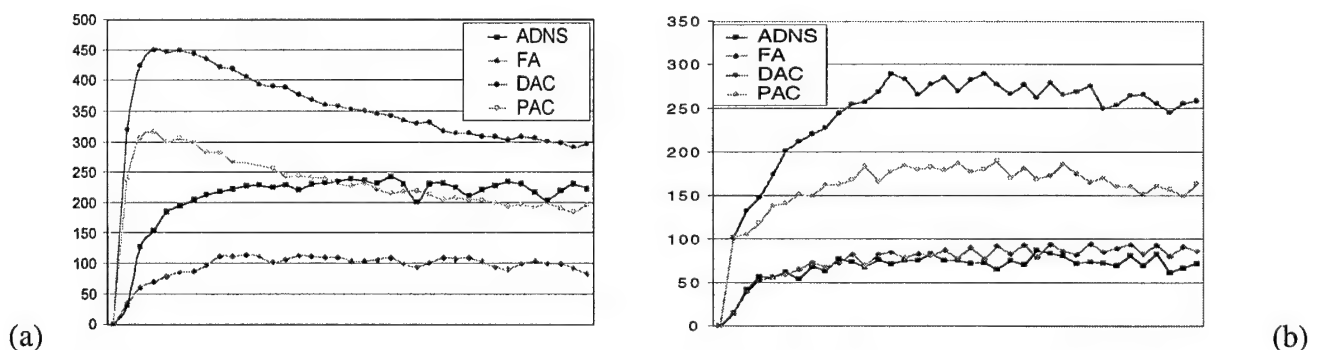|	Ductal AC	Papillary AC	FA	Adenosis
GR (cc/day)	0.06 ± 0.13	0.07 ± 0.14	0.03 ± 0.03	0.05 ± 0.06
Gd-DTPA-BMA @30s	122 ± 62	126 ± 68	39 ± 14	57 ± 22
Gd-DTPA-BMA @2min	251 ± 69	240 ± 75	145 ± 54	204 ± 65
Gadomer-17 @30s	47 ± 30	52 ± 23	23 ± 10	24 ± 11
Gadomer-17 @2min	92 ± 40	96 ± 32	51 ± 19	73 ± 22
Factor VIII MVD	**79 ± 19**	**70 ± 20**	**58 ± 18**	**53 ± 17**
VEGF H-score	134 ± 98	74 ± 68	126 ± 144	50 ± 76
TSP-1	62 ± 22	60 ± 23	57 ± 27	59 ± 21

(a)   (b)

Figure 10: Examples of Gd-DTPA-BMA (a) and Gadomer-17(b) enhancement kinetics for one papillary adenocarcinoma(PAC), one ductal adenocarcinoma(DAC), one adenosis(ADNS), and one fibroadenoma(FA). The malignant tumors had higher enhancements.

Discussion

A better characterization of this model may aid in future development of diagnostic or therapeutic agents tested on this model. As in human breast tumors, the enhancement kinetics of malignant tumors had a rapid up-slope, reaching to the maximum quickly, followed by a wash-out phase. The early enhancement is the best parameter to differentiate benign from malignant tumors. The immunohistochemical staining was used to measure the angiogenic biomarkers. The ductal adenocarcinoma had the highest microvessel density, then in order were papillary adenocarcinoma, fibroadenoma, and the adenosis had the lowest microvessel density, which was consistent with the degree of malignancy and benignity. MRI and IHC data were not correlated with each other, which may be due to the problem of tumor heterogeneity and non-matching sampling. However, MRI and IHC may provide different aspects (macroscopic and microscopic) complementing each other for assessment of tumor angiogenesis.

(6)   Key Research Accomplishments

- Carried out magnetic resonance imaging studies to monitor the taxotere treatment-induced effects in ENU induced tumors
- Developed the immunohistochemical methods to stain p53, TSP-1, CD31, Factor VIII, and VEGF in rat tissues
- Studied the IHC parameters in core needle biopsy samples and whole tumor specimens
- Correlate the MRI data with the IHC marker data using the specimens available from a previous study

(7)   Reportable Outcomes

- Two conference papers related to this project were presented.
- One journal paper was published

Conference Abstracts:

Min-Ying Su, Hon Yu, Jun Wang, Orhan Nalcioglu, "Characterization Of Angiogenesis in The Carcinogen ENU Induced Benign And Malignant Mammary Tumor Model" Second Era of Hope meeting (Department of Defense Breast Cancer Research Program Meeting), Orlando, FL, 2002

Min-Ying Su, Hon Yu, Jun Wang, Phillip Carpenter, John Fruehauf, and Orhan Nalcioglu, "Characterization of Angiogenesis in The Carcinogen ENU Induced Benign And Malignant Mammary Tumor Model". in "Proc., 11th ISMRM Annual Meeting, Toronto, 2003"

Journal Paper:
Min-Ying. Su, Hon Yu, Jr-Yuan Chiou, Jun Wang, John P. Fruehauf, Orhan Nalcioglu, Rita S. Mehta, and Choong Hyun Baick. Measurements of Volumetric Changes and Vascular Changes with Dynamic Contrast Enhanced MRI for Cancer Therapy Monitoring. Technology in Cancer Research and Treatment, **1**(6): 479-488, 2002.

(8)   Conclusions

This project was proposed to study the therapeutic indicators for anti-angiogenic therapy. The major effort in Yr-02 was spent on the ENU induced tumors. To date 46 mammary tumors were found. Every animal with mammary tumor was scheduled to receive a baseline MRI, core biopsy, then

followed by 4 treatments with weekly MRI follow-up. Only 25 rats (a total of 29 tumors, 4 rats had two tumors) had completed all designed studies. The tumors were categorized into responders, stabilizer, and non-responders depending on the final tumor size compared to the baseline size. The results obtained so far indicated that majority of infiltrating adenocarcinomas were responders and all papillary adenocarcinomas were stabilizer. The relationship between response and tumor type will be more clear when all data are available. In the responders, the Gd-DTPA-BMA enhancement at 2-min after injection showed a decreasing trend with treatment, which was not observed in the non-responders. However, the changes of MRI enhancement parameters with treatment did not show any significant differences among different response groups. We also completed the immunohistochemical staining study using available specimens of ENU induced tumors from another project. All tumors had wild type p53. The Factor VIII vessel density showed significance differences between malignant and benign tumors. The ductal adenocarcinoma had the highest microvessel density, then in order were papillary adenocarcinoma, fibroadenoma, and the adenosis had the lowest microvessel density, which was consistent with the degree of malignancy and benignity. The IHC study on the tumors undergoing chemotherapy are currently in progress. A no-cost extension has been filed to complete this study. All results will be summarized in the final report.

(9) Appendices

One abstract presented at second Era of Hope meeting, one abstract presented at the 11th ISMRM meeting, and one journal paper published in the "Technology in Cancer Research and Treatment" are enclosed.

CHARACTERIZATION OF ANGIOGENESIS IN THE CARCINOGEN ENU INDUCED BENIGN AND MALIGNANT MAMMARY TUMOR MODEL

Min-Ying Su, PhD, Hon Yu, MS, Jun Wang, MD, and Orhan Nalcioglu, PhD

Center for Functional Onco-Imaging, University of California, Irvine CA 92697-5020

E-mail: msu@uci.edu

As the potential of anti-angiogenic or anti-vascular therapy for cancer treatment becomes more promising, the development of valid animal models as well as therapeutic efficacy markers have become increasingly important. The carcinogen ENU can induce benign and malignant tumors in rats, and the malignant tumors came with various SBR (Scarff-Bloom-Richardson) grades, thus it can be used a suitable model for studies of differential diagnosis as well as malignant tumor grade staging. Assessment of angiogenesis by immunohistochemical (IHC) staining is the most commonly used technique. For each specimen we measured the expression level of mutant p53, thrombospondin-1, Vascular Endothelial Growth Factor (VEGF), and microvessel density using Factor VIII staining. On the other hand, imaging may be complementary to the IHC studies to measure the vascularity. In this study we characterized the angiogenesis status of the ENU induced mammary tumor model using Magnetic Resonance Imaging (MRI) and IHC molecular markers.

N-ethyl-N-nitrosourea (ENU, 90 mg/kg) was injected i.p. into 30-day old SPF Sprague-Dawley rats (n=50) to induce mammary tumors. The tumors started to appear 2 months after injection. The baseline MRI study was performed when the tumor reached approximately 1.0 cm in diameter. For each tumor the enhancement kinetics of two contrast agents, the small agent Gd-DTPA and a mid-sized agent Gadomer-17, were measured. The volumetric growth rates, as well as the early (30-sec) and maximum (approximately 2-min) enhancements between benign and malignant tumors were compared. Each tumor was then surgically removed for IHC staining analysis. The rats were kept for observation of recurrence, further development of other tumors, and metastasis into other organs, to explore whether this model can be used to study recurrence and metastasis as in human breast cancer.

Ninety three tumors were found in 1 year after the injection of ENU. Most tumors belonged to four major types, 2 malignant and 2 benign. The malignant tumors included ductal adenocarcinoma (n=25) and papillary adenocarcinoma (n=21), and the two major benign lesions were fibroadenoma (n=24) and adenosis (n=13). Multiple tumors (up to 5) could develop in one rat, all at different locations. Interestingly no tumor recurrence was observed at the surgical site after removal of a previous tumor. Also, none of the abdominal tumors were from breast origin. We also investigated lymph nodes from some rats, and found no sign of any cancer. In MRI studies, the two malignant tumors exhibited similar enhancement kinetics, showing rapid early enhancing slope and high enhancement magnitude. The two benign lesions had much slower early enhancing slope (highly significantly). In IHC studies, the ductal adenocarcinoma had the highest microvessel density, then in order was papillary adenocarcinoma, fibroadenoma, and the adenosis had the lowest microvessel density. All tumors had wild type p53. VEGF and TSP-1 were not significantly different among the 4 types. Higher vessel density was associated with higher MRI enhancement.

Our results demonstrated that all carcinogen ENU induced tumors were primary tumors, and they did not metastasize to lymph nodes or to other organs. A better characterization of this model may aid in future development of diagnostic or therapeutic agents tested on this model.

Characterization of Angiogenesis in The Carcinogen ENU Induced Benign And Malignant Mammary Tumor Model

Min-Ying Su, Hon Yu, Jun Wang, Phillip Carpenter[2], John Fruehauf[3], and Orhan Nalcioglu

Center for Functional Onco-Imaging and [2]Department of Pathology, University of California, Irvine, CA and [3]Oncotech Inc. Tustin, CA

Synopsis

Angiogenesis in carcinogen ENU-induced benign and malignant tumor models were studied with dynamic contrast enhanced MRI using two contrast agents (Gadodiamide and Gadomer-17). The tumors were then excised for immunohistochemical (IHC) staining to measure expression of angiogenic biomarkers, including mutant p53, TSP-1, VEGF, and Factor VIII microvessel density. Benign and malignant tumors had distinct contrast enhancement kinetics. Malignant tumors had a higher microvessel density than benign tumors. MRI and IHC may provide different aspects (macroscopic and microscopic) complementing each other for assessment of tumor angiogenesis.

Purpose

As the potential of anti-angiogenic or anti-vascular therapy for cancer treatment becomes more promising, the development of valid animal models as well as therapeutic efficacy markers have become increasingly important. The carcinogen ENU can induce benign and malignant tumors in rats, and the malignant tumors came with various SBR (Scarff-Bloom-Richardson) grades, thus it can be used as a suitable model for studies of angiogenesis. We applied dynamic contrast enhanced MRI and immunohistochemical (IHC) staining to study angiogenesis in the benign and malignant tumors of this model. Assessment of angiogenic biomarkers by immunohistochemical (IHC) staining is the most commonly used technique. For each specimen, we measured the expression level of mutant p53 (mp53), thrombospondin-1 (TSP-1), Vascular Endothelial Growth Factor (VEGF), and microvessel density (MVD) using Factor VIII staining. On the other hand, contrast enhanced imaging can be applied to measure the vascularity non-invasively. We utilized the broad spectrum of the ENU induced mammary tumor model and compared the angiogenesis measured using MRI and IHC molecular markers. Proper validation of imaging technique will facilitate its application in therapy monitoring, especially for anti-angiogenic or anti-vascular therapies.

Methods

N-ethyl-N-nitrosourea (ENU, 90 mg/kg) was injected i.p. into 30-day old SPF Sprague-Dawley rats (n=50) to induce mammary tumors. The tumors started to appear 2 months after injection. The baseline MRI study was performed when the tumor reached approximately 1.0 cm in diameter. For each tumor the enhancement kinetics of two contrast agents, the small agent Gadodiamide (Omniscan, 0.1 mmol/kg) and a mid-sized agent Gadomer-17 (0.05 mmol/kg, kindly provided by Schering AG, Germany), were measured. The volumetric growth rates, as well as the early (30-sec) and maximum (approximately 2-min) enhancements between benign and malignant tumors were compared. Each tumor was then surgically removed for IHC staining analysis to measure the expression of mp53, TSP-1, VEGF, and MVD. The rats were kept for observation of recurrence and further development of other tumors. The tumor types and angiogenesis of primary and subsequently developed tumors were compared.

Results

Ninety three tumors were found within 1 year after the injection of ENU. Most tumors belonged to four major types, 2 malignant and 2 benign. The malignant tumors included ductal adenocarcinoma (n=25) and papillary adenocarcinoma (n=21), and the two major benign lesions were fibroadenoma (n=24) and adenosis (n=13). Multiple tumors (up to 5) could develop in one rat, all at different locations. No tumor recurrence was observed at the surgical site after removal of a previous tumor. The subsequently developed tumors were not associated with the primary tumor. In MRI studies, two malignant tumors exhibited similar enhancement kinetics, showing rapid early enhancing slope and high enhancement magnitude. Figure 1 shows the enhancement kinetics measured by Gadodiamide (a) and Gadomer-17 (b) from these 4 tumor types. Two benign lesions had much slower early enhancing slope (highly significantly). The volumetric growth rates showed large variations even within each tumor type, and they were not correlated with the enhancement kinetics of both studied contrast agents. In IHC studies, the ductal adenocarcinoma had the highest microvessel density, then in order were papillary adenocarcinoma, fibroadenoma, and adenosis had the lowest microvessel density. All tumors had wild type p53. VEGF and TSP-1 were not significantly different among the 4 types. Higher vessel density was associated with higher MRI enhancement. Table 1 summarizes the growth rates, 30-sec and 2-min MR contrast enhancements and the IHC data.

Table 1: The growth rate, Gadodiamide and Gadomer-17 enhancements at 30-sec and 2-min and the IHC biomarkers: factor VIII microvessel density, VEGF histo-score and TSP-1 optical density in 4 tumor types

	Ductal AC	Papillary AC	FA	Adenosis
GR (cc/day)	0.06 ± 0.13	0.07 ± 0.14	0.03 ± 0.03	0.05 ± 0.06
Gadodiamide @30s	122 ± 62	126 ± 68	39 ± 14	57 ± 22
Gadodiamide @2min	251 ± 69	240 ± 75	145 ± 54	204 ± 65
Gadomer-17 @30s	47 ± 30	52 ± 23	23 ± 10	24 ± 11
Gadomer-17 @2min	92 ± 40	96 ± 32	51 ± 19	73 ± 22
Factor VIII MVD	**79 ± 19**	**70 ± 20**	**58 ± 18**	**53 ± 17**
VEGF H-score	134 ± 98	74 ± 68	126 ± 144	50 ± 76
TSP-1	62 ± 22	60 ± 23	57 ± 27	59 ± 21

Discussion

A better characterization of this model may aid in future development of diagnostic or therapeutic agents tested on this model. As in human breast tumors, the enhancement kinetics of malignant tumors had a rapid up-slope, reaching to the maximum quickly, followed by a wash-out phase. The early enhancement is the best parameter to differentiate benign from malignant tumors. The immunohistochemical staining was used to measure the angiogenic biomarkers. The ductal adenocarcinoma had the highest microvessel density, then in order were papillary adenocarcinoma, fibroadenoma, and the adenosis had the lowest microvessel density, which was consistent with the degree of malignancy and benignity. MRI and IHC data were not correlated with each other, which may be due to the problem of tumor heterogeneity and non-matching sampling. However, MRI and IHC may provide different aspects (macroscopic and microscopic) complementing each other for assessment of tumor angiogenesis.
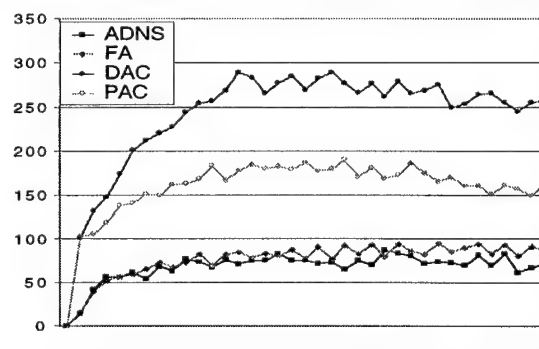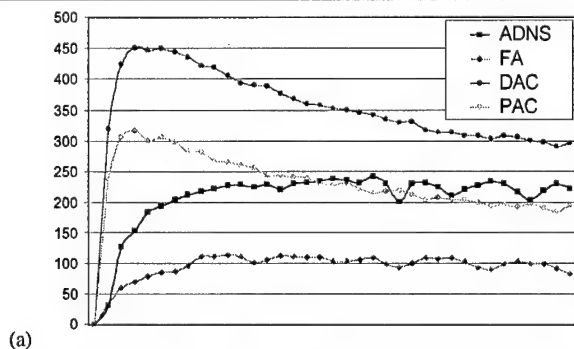

(a)   (b)

Figure 1: Examples of Gadodiamide (a) and Gadomer-17(b) enhancement kinetics for one papillary adenocarcinoma(PAC), one ductal adenocarcinoma(DAC), one adenosis(ADNS), and one fibroadenoma(FA). The malignant tumors had higher enhancements.

Measurement of Volumetric and Vascular Changes with Dynamic Contrast Enhanced MRI for Cancer Therapy Monitoring

www.tcrt.org

Min-Ying. Su, Ph.D.[1,*]
Hon Yu, M.S.[1]
Jr-Yuan Chiou, Ph.D.[1]
Jun Wang, M.D.[1]
Orhan Nalcioglu, Ph.D.[1]
John P. Fruehauf MD Ph.D.[2]
Rita S. Mehta, M.D.[3]
Choong Hyun Baick, M.D.[4]

[1]John Tu & Thomas Yuen Center for Functional Onco-Imaging
University of California
Irvine Hall 164
Irvine, CA 92697-5020, USA
[2]Oncotech Inc. Tustin, CA
[3]Department of Medicine, UC Irvine
[4]Department of Surgery, UC Irvine

Longitudinal dynamic contrast enhanced MRI studies were undertaken to monitor therapy induced volumetric and vascular changes. Three study components are presented in this work: one animal tumor chemotherapy study (R3230 AC adenocarcinoma treated with Taxotere), one patient with invasive lobular breast cancer undergoing neoadjuvant chemotherapy (AC regimen), and one patient with brain metastasis of primary breast cancer undergoing radiation therapy (40 Gray whole brain irradiation). In the animal study two contrast media with different molecular weights, Gadodiamide and Gadomer-17, were used. Only Gadomer-17 revealed significant changes in vascular properties. The responders showed decreased V_b (vascular volume index) and K_2 (out-flux transport rate), which preceded tumor regression. The control tumors showed increased V_b and K_2, before tumor growth became much faster. In the patient undergoing neoadjuvant therapy, the tumor was shrinking by 45% after 2 cycles of treatment, then again by 45% after 2 additional cycles. K_2 was decreasing over time with treatment. In the patient with brain metastasis, the 2 follow-up studies were much longer apart to monitor the regression and relapse of lesions. The pre-treatment volumes of lesions in the group without recurrence were significantly smaller compared to those with recurrence. In summary, the tumor volume was more sensitive than the vascular parameters measured by the small extracellular contrast medium for the assessment of therapy response and prediction of recurrence. The vascular properties measured by macromolecular contrast medium may have the potential to serve as early therapeutic efficacy indicators.

Key words: Contrast Enhanced MRI, Breast cancer, Chemotherapy, Radiation therapy, Therapy response

Introduction

Locally advanced breast cancer may be unresectable due to its invasion. Neoadjuvant chemotherapy may downstage the tumor, decrease the tumor size and render tumor resectable (1-2). Recent trend of breast conservation therapy encourages patients to receive down-staging neoadjuvant chemotherapy, even if cancers are readily operable, to avoid mastectomy or to improve prognosis (3-5). Furthermore, neoadjuvant chemotherapy may be used as an in vivo measure of tumor response to treatment, especially to evaluate the benefits of new treatment approaches (6-9). In parallel it has become increasingly important to develop reliable monitoring methods to measure the response of cancer at early times after the therapy is initiated. If therapy failure can be predicted early, it can be aborted to spare the patient from ineffective treatment and the associated morbidity. MRI provides great soft tissue contrast, and the post enhanced image after administration of contrast medium provides clear tumor margin for its delin-

* Corresponding Author:
Min-Ying Su, Ph.D.
Email: msu@uci.edu

479

eation, thus may be the best imaging modality for monitoring therapeutic response of breast cancer (10-14). When the enhancement kinetics is acquired dynamically, the vascular properties of the tumor can be obtained by performing pharmacokinetic analysis (15-16). Dynamic contrast enhanced MRI maybe applied longitudinally to reveal therapy induced vascular changes occurring in the tumor. In this study, we investigated whether the changes in the vascular parameters were associated with the final therapeutic response, thus might serve as early therapeutic indicators.

Three study components are included in this work. We first used an animal model (R3230 AC adenocarcinoma treated with Taxotere) for the development of study protocol and analysis methods. Pixel-by-pixel analysis was performed to handle the tumor heterogeneity problem (17). The pixel population distribution curves of vascular volume index (V_b) and vascular permeability index (out-flux transport rate K_2) were calculated. The longitudinal vascular changes were measured to determine whether they precede the volumetric changes of tumors, thus may serve as therapeutic indicators. In the animal study, we used two different contrast media, Gadodiamide (<1 kD) and Gadomer-17 (35 kD). It is known that the macromolecular contrast medium (MMCM) may reveal the vascular properties more accurately (18-19). The results obtained from the two contrast media were compared.

The same study protocol and the analysis methods were applied to two human studies: a patient with breast cancer receiving neoadjuvant chemotherapy (AC regimen), and a patient with metastatic breast cancer in the brain receiving radiation therapy. A pre-treatment and two follow-up studies were performed for each patient. In the breast cancer neoadjuvant therapy study, the volumetric changes and the vascular changes (V_b and K_2) occurring in the lesion after completing 2 cycles and 4 cycles of treatment were compared to investigate their relationship. In the brain metastasis radiation therapy study, the two follow-up studies were performed to measure remission and then relapse of lesions. The volume and the vascular properties of lesions in the baseline study were analyzed with respect to their recurrence status to investigate whether they can predict the recurrence.

Materials and Methods

Animal Tumor Chemotherapy Study

Nine female Fischer-344 rats (160 ~ 170 g) bearing the R3230 AC adenocarcinomas were used in the study. A small fragment of tumor harvested from a donor rat was implanted subcutaneously into a rat. When the tumor grew to 0.8 cm in diameter (approximately 3 weeks after implantation), the baseline MRI study was conducted. The animal MRI experiments were performed on a 3.0-T scanner using a Marconi

console (Cleveland, OH). One set of T2-weighted images covering across the tumor were acquired for volumetric measurements, using a fast spin echo sequence with TR=5500ms, TE=105.6 ms and 8 echo train. Then a T1-weighted sequence (RF-FAST VOL, with TR/TE = 18/3.6 ms and flip angle=20°) was used for the dynamic contrast enhancement study. A total of 40 acquisitions were prescribed. The temporal resolution was 24 sec for each acquisition. The contrast medium was injected as a short bolus after the first 4 acquisitions have been completed. In this animal study, two contrast media, an extracellular agent Gadodiamide (0.1 mmol Gd/kg Omniscan®, Nycomed Inc. Princeton, NJ) and a medium-sized agent Gadomer-17 (0.05 mmol Gd/kg), were injected sequentially. Gadomer-17 was a dendrimeric compound with size equivalent to a 35 kD protein, provided by Schering AG (Berlin, Germany). Firstly, Gadodiamide was injected and the enhancement kinetics were measured. After waiting 1 hour for the clearance of Gadodiamide, Gadomer-17 was injected and the enhancement kinetics were measured. After the baseline MRI was completed, six of the nine rats received i.v. injection of Taxotere (4 mg/kg, Aventis Pharmaceuticals Products Inc. Collegeville, PA) for chemotherapy. All rats were scanned at one week (week-1), two weeks (week-2) and three weeks (week-3) after the baseline study (week-0) for follow-up. The same imaging protocol with 2 sequentially injected contrast medium was used in all studies. The rats in the treated group received chemotherapy weekly, after each MRI study.

The total tumor volume was measured by manually outlining the tumor region on T2-weighted images. The viable tumor volume (determined as the enhanced tumor regions) was measured by threshold segmentation based on Gadodiamide enhanced images. The detailed procedure has been published previously (17). Figure 1a shows the growth curve of viable tumor volumes in 6 rats. It can be seen that the largest difference between controls and treated tumors happened at week-3. The ratio of week-3 volume divided by week-2 volume was used to categorize the degree of responses, as shown in Figure 1b. Those tumors shrinking between week-2 and week-3 were categorized as responders, and those still growing but at a slower rate compared to the controls were categorized as partial responders (not shown in Fig. 1a). Three of the six treated rats were classified as responders (with week-3/week-2 growth ratios of 0.82, 0.88 and 0.88), whereas the other three treated rats were classified as partial responders as their ratios were greater than 1 (1.07, 1.22 and 1.26), but still lower than the control group's ratios (1.92, 1.93 and 2.24). Since the most volumetric group differences happened between week-2 and week-3, we were interested in measuring changes in the enhancement kinetics prior to the changes in tumor volume occurred, i.e. between week-1 and week-2. In addition to the overall enhancement kinetics, the changes in the pixel population distribution curves of
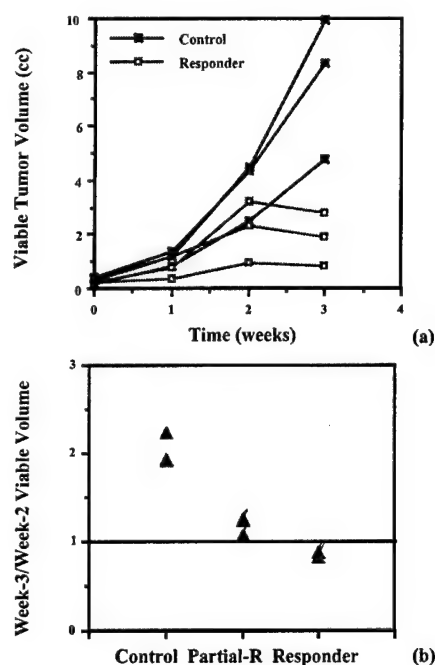
Figure 1: The growth curve of the viable tumor volume in 3 control and 3 responder rats. The most difference happened at wek-3. The ratio between week-3 and week-2 viable tumor volume was used to separate responders (ratio <1: 0.82, 0.88, 0.88) and partial responders (ratio >1: 1.07, 1.22, 1.26) from controls (1.92, 1.93, 2.24).

pharmacokinetic parameters were measured. All pixels contained within the viable region of each tumor were analyzed on a pixel-by-pixel basis by using a 2-compartmental pharmacokinetic model, as described next.

Pharmacokinetic Analysis and Pixel Population Distribution

A 2-compartmental model can be used to describe the transport of contrast medium in tissue vascular and interstitial spaces as a function of time, which allows the determination of the relative tracer concentration in these two tissue compartments. The details of the methodology have been described in previous publications (20-21). Briefly, the transport of tracer from the plasma compartment into the extravascular compartment can be expressed as Eq. [1].

$$V_e \frac{dC_e}{dt} = k_1 C_p - k_2 C_e \qquad 1(a)$$

$$\text{or} \qquad \frac{dC_e}{dt} = K_1 C_p - K_2 C_e \qquad 1(b))$$

where K_1 and K_2 are defined as $K_1 \equiv k_1 / V_e$, and $K_2 \equiv k_2 / V_e$. C_p and C_e are the tracer concentrations in the plasma and extravascular compartments, V_e is the distribution volume of

the contrast medium in the extravascular extracellular space, k_1 is the in-flux transport rate from plasma to interstitial space, and k_2 is the out-flux transport rate from interstitial space back into plasma. K_1 and K_2 are the transport constants related to the leakage space, whereas k_1 and k_2 are related to whole tissue. Total enhancement kinetics constituted the contributions from both the vascular and the extravascular compartments. The total concentration in a selected region of interest in tissue, C_T, is from the contributions of both plasma and extravascular compartments, as shown in Eq. [2].

$$C_T(t) = V_p \cdot C_p(t) + V_e \cdot C_e(t) = V_b \cdot C_b(t) + V_e \cdot C_e(t) \qquad [2]$$

where C_p is the contrast medium concentration in plasma, which is related to (Gd) in blood by $C_b = C_p(1\text{-Hct})$, Hct = hematocrit, V_p is the plasma volume fraction (blood volume $V_b = V_p/(1\text{-Hct})$), and V_e is the leakage space fraction in the selected ROI.

A Non-Linear Least squares (NLLS) fitting was applied to analyze the measured enhancement kinetic curve, for obtaining three independent fitting parameters from the best fit. These three parameters were: the apparent vascular volume (V_b), the product of the in-flux transport rate and the distribution volume in the interstitial space $(V_e K_1)$, and the out-flux transport rate (K_2). The analysis process was similar to that described by Tofts, who proposed a unified model that reconciles various models proposed by different research groups (15). Our notation $V_e K_1$ is equivalent to (kin$^{PS\rho}$), and K_2 is equivalent to (kout$^{PS\rho}/V_e$) used in the unified model.

The enhancement kinetics from each pixel was measured then fitted with the pharmacokinetic model to obtain the vascular volume (V_b) and the out-flux transport rate (K_2). For each parameter, the values from all pixels of 3 tumors in each study group were pooled together and sorted in a descending order, then the cut-off values of the top 90% pixels, 80% pixels, 10% pixels were determined to generate the pixel population distribution curve. The detailed procedure has been published previously (17).

Monitoring Neoadjuvant Chemotherapy in A Patient with Breast Cancer

The similar study protocol and analysis methods used for the animal study were used for the human study. Dynamic contrast enhanced MRI was applied to monitor the efficacy of neoadjuvant chemotherapy in a 48-year-old women with invasive lobular breast cancer. The MRI scan was performed on a 1.5 Tesla Marconi Eclipse system (Cleveland, OH) with a dedicated breast coil. The dynamic acquisition was performed using a 3D gradient echo pulse sequence (RF-FAST VOL) with TR/TE = 10/3.6 ms, flip angle = 20°, and acquisition

matrix = 256×128. The temporal resolution was 42 sec for one acquisition. The FOV (Field of view) was 32 cm. Thirty-two slices with 4 mm thickness were used to cover both breasts. Sixteen frames were prescribed. The contrast medium Gadodiamide (1cc Omniscan® per 10 lbs body weight, Nycomed Inc. Princeton, NJ) was injected after 4 acquisitions were completed. The post contrast images were acquired for the next 12 frames, lasting approximately 8 minutes after injection. After the baseline MRI, the patient received AC regimen chemotherapy (Adrimycine and Cyclophosphamide). The follow-up MRI exam was performed at 2 weeks after completing 2 cycles, then again at 2 weeks after completing 4 cycles to measure the therapy induced changes.

The analysis was similar to that used in animal studies. The tumor regions were determined from contrast enhancement maps. The color-coded enhancement maps were obtained by subtracting the mean pre-contrast image (averaged over the first 4 frames) from the 2-min post enhanced image (the 8th frame). The color-coding scale was fixed in the analysis of all 3 MRI studies, so that the tumor regions could be determined with a consistent criterion. The enhancement maps of one slice containing a tumor mass in the 3 MRI studies are shown in Figure 2a. It clearly demonstrated that the tumor was shrinking. A boundary covering the entire bilateral breast region was drawn for the pixel-by-pixel analysis. The enhancement kinetics of all pixels contained within this boundary were measured, then analyzed with the pharmacokinetic model to obtain the parameters. These fitted parameters were then used to construct the pharmacokinetic maps, shown in Figure 2b for V_b and Figure 2c for K_2. The fitting parameters obtained from all tumor pixels were separately obtained to calculate the pixel population distribution curves. The V_b and K_2 curves in the pre-treatment and the 2 post-treatment studies were compared.

Assessment of Recurrence in A Patient with Metastatic Breast Cancer in the Brain

The similar study protocol was applied to study one female patient (54-year-old) with metastatic breast cancer in the brain. A baseline MRI was performed before initiation of radiation therapy. Then the patient received 40 Gray whole brain radiation therapy for 4 weeks. A follow-up MRI was performed at 2 months after the radiation therapy was completed. Almost all metastatic lesions in the first follow-up study disappeared, thus the changes in the enhancement kinetics were not assessed. Then 6 months later the third MRI was performed to examine the recurrence of brain metastasis. Therefore, in this study instead of investigating the therapy induced short-term changes, we were interested in studying the indicators for recurrence. The dynamic contrast enhanced MRI was acquired using the same 3D gradient echo pulse sequence (RF-FAST VOL). The parameters were:

coronal view, TR = 10 ms, TE = 3.63 ms, flip angle = 20 degree, slice thickness = 6 mm, FOV = 22 cm, image matrix = 256×128×28, number of frames = 16. The temporal resolution for each acquisition was 34 sec. Since many small lesions were identified, image registration was required to locate the corresponding lesions in different studies. The realignment program provided in SPM99 (Statistical Parametric Mapping, Developed by members & collaborators of the Wellcome Department of Cognitive Neurology, UK) was used to register the set of 3D images taken in the follow-up studies to those in the baseline study. Figure 3a shows the realigned contrast enhanced images from 4 consecutive slices (columns) acquired in 3 studies (rows). As noted in the figure, 7 lesions were identified from these 4 slices in the baseline study. Most lesions disappeared or became very small with a much lower contrast enhancement at the 3-month follow-up study (2 months after completing radiation therapy). Six months later in the second follow-up study, some lesions did not recur, some recurred but with a small size, and some lesions were with a large size, even bigger than their initial size in the baseline study.

Table I

The volumes of 7 lesions in the baseline and the 2nd follow-up studies in Figure 3

Lesions	Baseline volume (cc)	2nd follow-up volume (cc)
1	0.45	0.44
2	0.96	0.08
3	1.20	1.18
4	0.26	0
5	0.50	0
6	0.97	0
7	1.28	0.07

The color-coded enhancement maps were obtained, and from which the tumor region was outlined to measure the volume of each lesion. Figure 3b shows the corresponding enhancement maps of the 4 slices. The darker reddish color represents a higher enhancement. Only lesions exhibiting red enhancement color was counted. Some larger lesions were found to extend into the neighboring slices. By carefully examining their relative locations, we could identify whether a lesion shown on one slice was a separate lesion or was a part of a lesion from the previous slice. All together, 32 lesions were identified in the baseline study. The volumes of the 7 identified lesions shown in Figure 3 in the baseline and the second follow-up studies are listed in Table I. Lesions 4, 5 and 6 did not recur. Lesions 2 and 7 recurred but with a much smaller volume. Lesions 1 and 3 recurred to their baseline sizes. In addition to the volume, the enhancement kinetics of all lesions were analyzed using the same pharmacokinetic analysis methods. For each lesion, the enhancement kinetics of all pixels were measured, then analyzed with the pharmacokinetic model to calculate the pixel population distribution curves of V_b and K_2. We were interested in investigating which baseline characteristics of the lesion (volume,
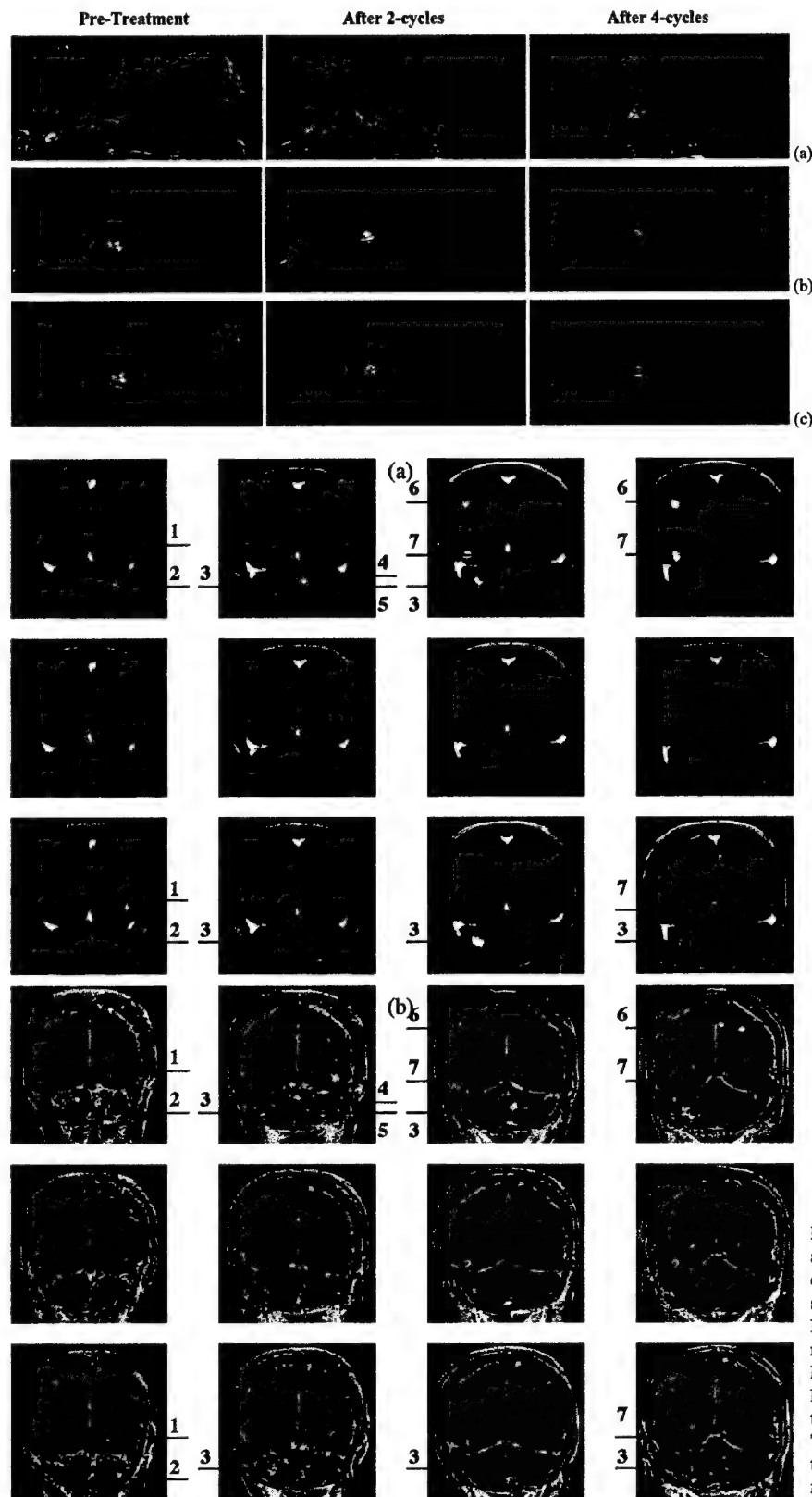
Figure 2: The color-coded enhancement maps (a) of one imaging slice containing a tumor mass in the pre-treatment study and the 2 follow-up studies after completing 2 cycles and 4 cycles treatment. The darker reddish color represents a higher enhancement. The color-coding scale was identical in the 3 MRI studies. The tumor was shrinking with treatment. Pixel-by-pixel pharmacokinetic analysis was performed to obtain the reconstructed V_b (b) and K_2 (c) maps.

V_b and K_2 profile) were associated with the recurrence, thus may be used to predict the recurrence status.

Results

Animal Tumor Chemotherapy Study

The tumor bearing animals tolerated the Taxotere chemotherapy well. However, the therapy did not cause a substantial effect on the R3230 AC adenocarcinoma resulting in shrinkage. The treated tumors showed a slower growth rate compared to the controls. The most difference between control and treated tumors occurred between week-2 and week-3, thus it was used to separate responders and partial responders from controls. The changes in the tumor enhancement kinetics between week-1 and week-2 (before the volumetric change occurred) were studied. Figure 4 shows the pixel population distribution curve of V_b for the control group (Fig. 4a) and the responder group (Fig. 4b) measured with Gadomer-17 at

Figure 3: The contrast enhanced images (a) and the color-coded enhancement maps (b) of 4 consecutive imaging slices in the baseline study before treatment (1st row), the first follow-up study when the lesions regressed (2nd row), and the second follow-up study when the lesions relapsed (3rd row). For some large lesions extending into the neighboring slices, they could be identified by the relative location. The volumes of each lesion in the baseline and the second follow-up studies were measured from the color-coded enhancement maps.

week-1 and week-2. In the control group the V_b curve at week-2 was increased throughout the whole population compared to the curve at week-1 (significant from 10th to 70th percentile); whereas in the responder group the distribution at week-2 was reduced with respect to its week-1's curve throughout the whole population (significant from 30th to 70th percentile). Figures 5a and 5b show the pixel population distribution curves of K_2 at week-1 and week-2 measured with Gadomer-17 for the control and responder groups, respectively. In the control group the K_2 was increased throughout the population (significant from 20th to 80th percentile). Interestingly that was associated with the much faster growth of tumors subsequently from week-2 to week-3. In contrast the responders showed decreased K_2, but it was not statistically significant. The changes in the V_b and K_2 profiles from week-1 to week-2 were opposite between controls and responders. The partial responder group showed an increased V_b at week-2 with respect to week-1's and showed a decreased K_2. Similar procedures were performed to analyze the enhance-ment kinetics measured by the smaller extracellular agent Gadodiamide. The V_b and K_2 distribution curves did not show any significant changes among these 3 groups.

Monitoring Neoadjuvant Chemotherapy in A Patient with Breast Cancer

In the breast patient study only the clinically approved small contrast medium Gadodiamide was used. Three MRI studies were performed, one pre-treatment and 2 follow-up's at 2 weeks after 2 cycles of treatment and 2 weeks after 4 cycles of treatment. The biopsy results showed that the patient had confirmed multi-focal lobular cancers at 2 different sites. The image slice shown in Figure 2 only covered one mass at one site. The volumes of this mass were 3.7 cc at baseline, 2.0 cc after 2-cycles of treatment and 1.1 cc after 4-cycles of treatment. The tumor shrank by 45% after 2-cycles, then again shrank by 45% after 2 more cycles. The other mass connecting to this one, and the tumor at another site all
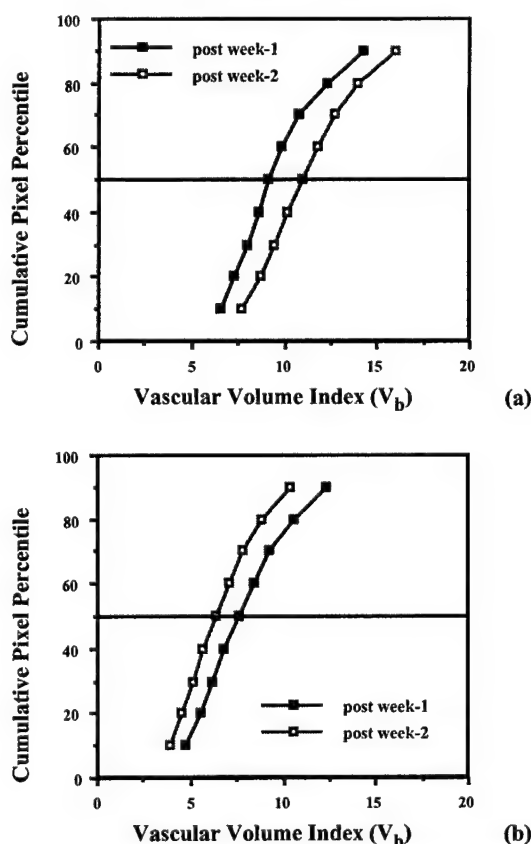

Figure 4: The pixel population distribution curves of the vascular volume index (V_b) in the control (a) and the responder (b) groups at week-1 and week-2. In the control group, the V_b shifted to higher values at week-2 throughout the entire population; whereas in the responder group the V_b was reduced at week-2 compared to week-1.
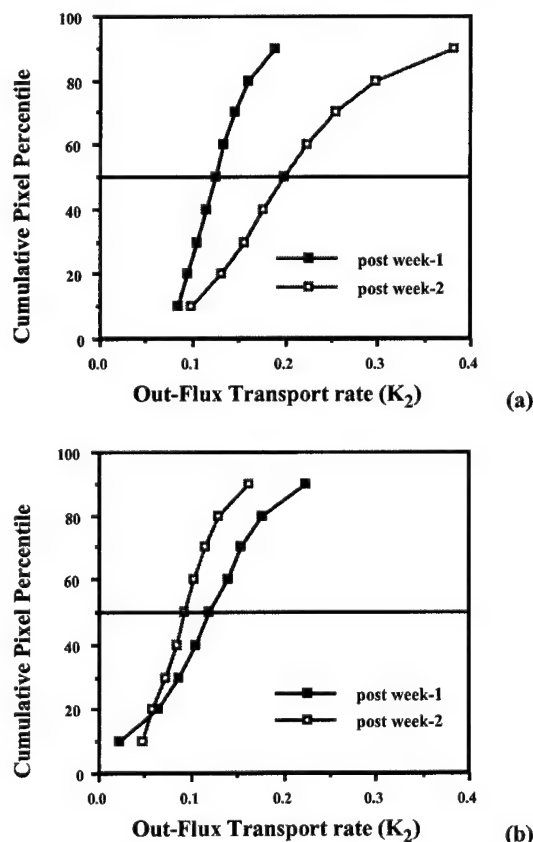
Figure 5: The pixel population distribution curves of the out-flux transport rate (K_2) in the control (a) and the responder (b) groups at week-1 and week-2. In the control group, the K_2 was increased at week-2 throughout the entire population. Interestingly that was associated with the much faster growth rate subsequently between week-2 and week-3 (shown in Fig. 1a). In the responder group the K_2 was reduced at week-2 compared to week-1.

showed similar responses and a comparable shrinkage rate. Figure 6a shows the enhancement kinetics measured from this mass at the 3 time points, using the region of interest analysis covering the entire mass. The baseline kinetics had the highest magnitude and a clear wash-out phase. The magnitude of enhancement decreased with treatment. All pixels contained within this mass were analyzed on a pixel-by-pixel basis, then the V_b and K_2 population distribution curves were calculated. The V_b and K_2 curves in the 3 MRI studies

are shown in Figure 6b and 6c, respectively. In the V_b distribution profile, the pre-treatment and the post 2-cycles studies had similar curves, and the post 4-cycles study had substantially lower V_b values. In the K_2 distribution profile, it demonstrated a reduced K_2 over time with treatment. For all analyzed parameters, the tumor volume was the one showing the highest percentage change with treatment.

Assessment of Recurrence in A Patient with Metastatic Breast Cancer in the Brain
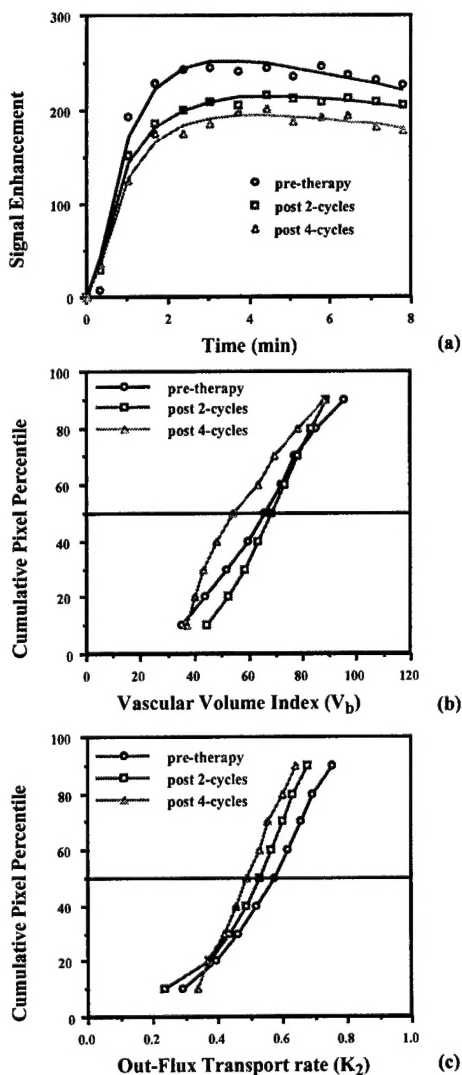

Figure 6: The contrast enhancement kinetics (a) measured from the mass shown in Figure 2 at three time points. The lesion exhibited a slower upslope and lower enhancement magnitude after receiving treatment. The wash-out rate became flattened after treatment. Pixel-by-pixel analysis was performed to obtain the population distribution curve of V_b (c) and K_2 (c) in all 3 MRI studies. The V_b was reduced at post 4-cycles, and the K_2 was decreasing with treatment.
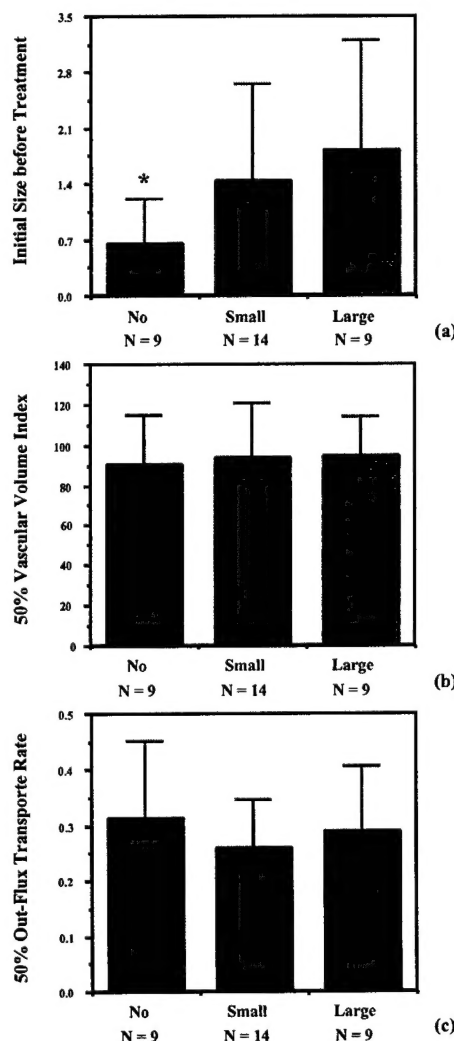
Figure 7: Thirty-two brain metastatic lesions identified in the baseline study were separated into three groups according to their recurrence size (no recurrence, volume < 0.45, or volume > 0.48) in the second follow-up study. The baseline volume (a) and the median V_b (b) and median K_2 (c) of lesions in each group are shown. The error bar represents the standard deviation. Only the baseline volume was associated with the recurrence status (significantly lower in the no-recurrence group).

In this brain metastasis study similarly three MRI studies were performed, one before radiation therapy, and 2 follow-up's at 2 months and 8 months after completing a treatment regimen of 4-weeks-long 40 Gray whole brain irradiation. By carefully examining the relative location of all lesions shown on contrast enhanced images, 32 separate lesions were identified in the baseline study. In the first follow-up study, these lesions either totally disappeared or became very small and showed a much lower enhancement. In the second follow-up study, some lesions recurred, some did not, and also some new lesions appeared. By co-registering all images in the 3 studies, we were able to match the lesion locations to determine the recurrence size of each of the 32 lesion. Nine lesions did not recur; 14 lesions recurred with a volume less than 0.45 cc; and 9 lesions recurred with a volume greater than 0.48 cc. The largest recurrence lesion size was 4.0 cc. According to their recurrence size, the 32 baseline lesions were separated into 3 groups. The baseline volume and the enhancement kinetics of all lesions in each group were measured then compared between groups. Figure 7a shows the baseline volumes of lesions in these 3 groups. The group without recurrence had a significantly smaller volume (0.65 ± 0.55 cc) than the group with small recurrence (1.45 ± 1.20 cc) or the group with large recurrence (1.83 ± 1.37 cc). The difference between the later 2 groups was not significant. The enhancement kinetics of all pixels contained within each lesion were measured then analyzed with the pharmacokinetic model to obtain the V_b and K_2 population distribution curves. The median V_b and K_2 of each lesion was obtained for statistical analysis. Figures 7b and 7c show the mean value of the median V_b and K_2 for the 3 groups, respectively. Apparently there was no difference in the baseline median V_b or median K_2 of lesions in these 3 groups. Similar analysis was performed for all pixel percentile values (10th to 90th). None of these V_b or K_2 values showed significant differences among the three groups.

Discussion

We reported three studies in this work, an animal tumor chemotherapy study, a human breast cancer neoadjuvant chemotherapy study, and a human metastatic breast cancer radiation study. The similar study protocol and analysis methods were used in all 3 studies. The only difference was that in the animal study we could use a medium-sized macromolecular agent Gadomer-17. This agent is not an FDA approved agent for human study. Pre-treatment and follow-up studies were performed to measure the changes of tumor volumes and the vascular properties over time. In the first 2 chemotherapy studies, the relationship between volumetric changes and vascular changes were investigated. If earlier vascular changes were associated with subsequent volumetric changes, then they may serve as early therapeutic indicators to predict final outcome. The nature of the radiation

therapy study was different from the 2 chemotherapy studies. The follow-up times were longer to study remission (1st follow-up, 2 months after completing radiation therapy) then relapse (2nd follow-up, 6 months after the 1st follow-up) of brain metastasis. We investigated whether the baseline lesion volume or the vascular properties were associated with the recurrence status. If such relationships can be found, one may predict which lesion is more likely to recur.

In the animal studies the tumors were separated into responders and partial-responders according to their volumetric growth curves (Fig. 1). Since the largest volumetric differences happened between week-2 and week-3, the changes of vascular properties between week-1 and week-2 were of interest. The vascular volume index (V_b) and the permeability index (K_2) measured by Gadomer-17 showed significant changes between controls and responders. In the control group, the V_b and the K_2 (Figs. 4a and 5a) increased from week-1 to week-2, which was associated with the much faster growth rate between week-2 and week-3 (Fig. 1a). In the responder group the V_b and K_2 decreased (Figs. 4b and 5b), which was associated with the subsequent regression between week-2 and week-3 (Fig. 1a). In the partial responder group the V_b increased from week-1 to week-2 but the K_2 decreased. The partial responder tumors still grew between week-2 and week-3 but at a much slower rate compared to control tumors. The results suggest that the early vascular changes in V_b and K_2 as measured by a macromolecular contrast agent such as Gadomer-17 could possibly serve to predict the treatment efficacy. Similar analysis was performed to analyze the vascular properties measured by the small extracellular agent Gadodiamide. But not any significant changes were observed between groups. The results were consistent with the findings reported in an earlier publication studying R3230 AC tumor receiving Mitomycinc-C chemotherapy (17). The utility of macromolecular contrast medium (MMCM)-enhanced MRI for tumor angiogenesis characterizations has been established experimentally in a range of cancer types including breast, ovary, fibrosarcoma, and prostate (22).

In the human breast cancer neoadjuvant chemotherapy, the volumetric shrinkage was the most pronounced feature among all parameters analyzed. The lesion shown in Figure 2 showed a 45 % reduction in size for every 2 cycles of treatment. The enhancement kinetics measured from the remaining lesion showed a slower up-slope, a lower enhancement magnitude, and a flattened wash-out phase after treatment (Fig. 5a). The enhancement kinetics was greatly dependent on the region of interest covering the lesion. In our analysis the tumor region was outlined based on color-coded enhancement maps obtained at 2-min post contrast injection (Fig. 2b). A consistent color-coding scale was used in all 3 MRI studies. Only regions showing a red color coding were included in the tumor ROI. Therefore, it was not surprisingly that the

enhancement kinetics did not show substantial changes. If the tumor ROI in the follow-up studies enclosed a larger region with lower enhancements, then the volumetric shrinkage rate would be smaller, and the changes in the enhancement kinetics would be greater. In the pharmacokinetic analysis, a reduced V_b in the second follow-up study (Fig. 5b), and a trend of decreasing K_2 over time with treatment (Fig. 5c) were observed. The percentage changes in V_b and K_2 were much smaller than the percentage change in tumor volume. Since only one case study was presented, significance of this result could not be determined. The same protocol will have to be applied to study a cohort of patients, then the appropriate statistical analysis can be performed to assess the potential of using vascular properties to predict final therapy outcome.

Several studies employing contrast enhanced MRI for monitoring neoadjuvant chemotherapy in breast cancer have been reported. Gilles *et al.* studied 18 patients and showed that early enhancement correlated well with pathological residual tumor (10). Abraham *et al.* applied RODEO MRI technique to determine tumor response and the extent of residual disease in 39 patients, and concluded that MRI performed better than traditional methods of physical exam or mammogram in assessment of response (12). Trecate *et al.* used dynamic contrast enhanced MRI to exam 30 patients, and reported an overall accuracy of 90% (13). Rieber *et al.* reported a series of 58 patients (14). Tumor size and the dynamic contrast medium uptake pattern were evaluated and compared with the final histological findings. The diagnostic accuracy for assigning patients to the non-response (NR) group was 83.3 % and to the partial response (PR) group was 82.4%, but the determination of residual tumor size was unreliable in the complete response (CR) group. Esserman *et al.* investigated the association between MRI phenotype of breast lesions and response to neoadjuvant chemotherapy (23). The circumscribed mass is more likely to respond to therapy (77%) than the other patterns (20-37.5%). No reports are available yet investigating early therapeutic indicators in breast cancer receiving neoadjuvant chemotherapy. In patients with bone or soft-tissue sarcomas, it has been demonstrated that the extent of tumor necrosis and viability measured by dynamic MRI may serve as early predictors for the efficacy (24-25).

In the radiation therapy study the baseline lesion characteristics, including volume and vascular properties, were analyzed with respect to the recurrence status. Similarly, the first step was to determine the tumor region. The color-coded enhancement maps provided a consistent reference for the ROI outlining. The baseline lesion volume was the only parameter showing a significant difference between lesions with and without recurrence. Hawighorst *et al.* reported a study using serial MRI to assess the response of brain metastasis of different primaries receiving radiosurgery and concluded that MRI is a sensitive imaging tool to evaluate tumor response (26). In another study, they used longitudinal pharmacokinetic MRI to monitor the response of malignant brain glioma to stereotactic radiotherapy (27). It was found that a low enhancement amplitude before therapy, combined with an early drop of K_{21} after therapy, can reliably predict subsequent tumor shrinkage. More studies are needed to define the role of longitudinal dynamic contrast enhanced MRI in assessment or prediction of the response of brain metastasis to radiotherapy.

Summarizing from all three studies reported in this work, the changes in tumor size seemed to be the most sensitive response to treatment and to predict recurrence. Contrast enhanced images are definitely required for the tumor volumetric delineation, but the pharmacokinetic vascular properties analyzed from dynamic contrast enhancement studies did not seem to provide additional useful information for monitoring therapy efficacy in human studies. This may due to the use of smaller molecular weight contrast agent (Gadodiamide), that extravasates rapidly into the interstitial space. When the macromolecular contrast media are approved for clinical use, they may provide useful early indicators which are associated with the final therapeutic outcome, as demonstrated in our animal study.

In this study the pharmacokinetic analysis was performed on a pixel-by-pixel basis to handle the problem of tumor heterogeneity. The pixel population distribution curve allows the analysis in the entire population spectrum or in a certain subgroup of pixels. Whether the subpixel population analysis can provide useful information to predict therapy outcome will have to be determined in a study involving larger number of patients.

References

1. Gianni, L., Valagussa, P., Zambetti, M., Moliterni, A., Capri, G., Bonadonna, G. Adjuvant and neoadjuvant treatment of breast cancer. *Semin. Oncol. 28*, 13-29 (2001).
2. Cance, W. G., Carey, L. A., Calvo, B. F., Sartor, C., Sawyer, L., Moore, D. T., Rosenman, J., Ollila, D. W., Graham, M. Long-term outcome of neoadjuvant therapy for locally advanced breast carcinoma: Effective clinical downstaging allows breast preservation and predicts outstanding local control and survival. *Ann. Surg. 236*, 295-303 (2002).
3. Bonadonna, G., Valagussa, P., Brambilla, C., Ferrari, L., Moliterni, A., Terenziani, M., Zambetti, M. Primary chemotherapy in operable breast cancer: Eight-year experience at the Milan Cancer Institute. *J. Clin. Oncol. 16*, 93-100 (1998).

4. Wolff, A. C., Davidson, N. E. Early operable breast cancer. *Curr. Treat. Options. Oncol. 1*, 210-220 (2000).

5. Wolff, A. C., Davidson, N. E. Preoperative therapy in breast cancer: Lessons from the treatment of locally advanced disease. *Oncologist 7*, 239-245 (2002).

6. Sapunar, F., Smith, I. E. Neoadjuvant chemotherapy for breast cancer. *Ann. Med. 32*, 43-50 (2000).

7. Stebbing, J. J., Gaya, A. The evidence-based use of induction chemotherapy in breast cancer. *Breast Cancer 8*, 23-37 (2001).

8. Aapro, M. S. Neoadjuvant therapy in breast cancer: Can we define its role? *Oncologist Suppl 3*, 36-39 (2001).

9. Smith, I. E., Lipton, L. Preoperative/neoadjuvant medical therapy for early breast cancer. *Lancet Oncol. 2*, 561-570 (2001).

10. Gilles, R., Guinebretiere, J. M., Toussaint, C., Spielman, M., Rietjens, M., Petit, J. Y., Contesso, G., Masselot, J., Vanel, D. Locally advanced breast cancer: Contrast-enhanced subtraction MR imaging of response to preoperative chemotherapy. *Radiology 191*, 633-638 (1994).

11 Knopp, M. V., Brix, G., Junkermann, H. J., Sinn, H. P. MR mammography with pharmacokinetic mapping for monitoring of breast cancer treatment during neoadjuvant therapy. *Magn. Reson. Imaging Clin. N. Am. 2*, 633-658 (1994).

12. Abraham, D. C., Jones, R. C., Jones, S. E., Cheek, J. H., Peters, G. N., Knox, S. M., Grant, M. D., Hampe, D. W., Savino, D. A., Harms, S. E. Evaluation of neoadjuvant chemotherapeutic response of locally advanced breast cancer by magnetic resonance imaging. *Cancer 78*, 91-100 (1996).

13. Trecate, G., Ceglia, E., Stabile, F., Tesoro-Tess, J. D., Mariani, G., Zambetti, M., Musumeci, R. Locally advanced breast cancer treated with primary chemotherapy: Comparison between magnetic resonance imaging and pathologic evaluation of residual disease. *Tumori 85*, 220-228 (1999).

14. Rieber, A., Brambs, H. J., Gabelmann, A., Heilmann, V., Kreienberg, R., Kuhn, T. Breast MRI for monitoring response of primary breast cancer to neo-adjuvant chemotherapy. *Eur. Radiol. 12*, 1711-1719 (2002).

15. Tofts, P. S. Modeling tracer kinetics in dynamic Gd-DTPA MR imaging. *J. Magn. Reson. Imaging. 7*, 91-101 (1997).

16. Tofts, P. S., Brix, G., Buckley, D. L., Evelhoch, J. L., Henderson, E., Knopp, M. V., Larsson, H. B., Lee, T. Y., Mayr, N. A., Parker, G. J., Port, R. E., Taylor, J., Weisskoff, R. M. Estimating kinetic parameters from dynamic contrast-enhanced T(1)-weighted MRI of a diffusable tracer: Standardized quantities and symbols. *J. Magn. Reson. Imaging. 10*, 223-232 (1999).

17. Su, M. Y., Wang, Z., Nalcioglu, O. Investigation of longitudinal vascular changes in control and chemotherapy-treated tumors to serve as therapeutic efficacy predictors. *J. Magn. Reson. Imaging. 9*, 128-137 (1999).

18. van Dijke, C. F., Brasch, R. C., Roberts, T. P., Weidner, N., Mathur, A., Shames, D. M., Mann, J. S., Demsar, F., Lang, P., Schwickert, H. C. Mammary carcinoma model: Correlation of macromolecular contrast-enhanced MR imaging characterizations of tumor microvasculature and histologic capillary density. *Radiology 198*, 813-818 (1996).

19. Daldrup, H., Shames, D. M., Wendland, M., Okuhata, Y., Link, T. M., Rosenau, W., Lu, Y., Brasch, R. C. Correlation of dynamic contrast-enhanced MR imaging with histologic tumor grade: Comparison of macromolecular and small-molecular contrast media. *AJR Am. J. Roentgenol. 171*, 941-949 (1998).

20. Su, M. Y., Jao, J. C., Nalcioglu, O. Measurement of vascular volume fraction and blood-tissue permeability constants with a pharmacokinetic model: Studies in rat muscle tumors with dynamic Gd-DTPA enhanced MRI. *Magn. Reson. Med. 32*, 714-724 (1994).

21. Su, M. Y., Muhler, A., Lao, X., Nalcioglu, O. Tumor characterization with dynamic contrast-enhanced MRI using MR contrast agents of various molecular weights. *Magn. Reson. Med. 39*, 259-269 (1998).

22. Brasch, R., Turetschek, K. MRI characterization of tumors and grading angiogenesis using macromolecular contrast media: Status report. *Eur. J. Radiol. 34*, 148-155 (2000).

23. Esserman, L., Kaplan, E., Partridge, S., Tripathy, D., Rugo, H., Park, J., Hwang, S., Kuerer, H., Sudilovsk, D., Lu, Y., Hylton, N. MRI phenotype is associated with response to doxorubicin and cyclophosphamide neoadjuvant chemotherapy in stage III breast cancer. *Ann. Surg. Oncol. 8*, 549-559 (2001).

24. Fletcher, B. D., Hanna, S. L., Fairclough, D. L., Gronemeyer, S. A. Pediatric musculoskeletal tumors: Use of dynamic, contrast-enhanced MR imaging to monitor responses to chemotherapy. *Radiology 184*, 243-248 (1992).

25. Bonnerot, V., Charpentier, A., Frouin, F., Kalifa, C., Vanel, D., Di Paola, R. Factor analysis of dynamic magnetic resonance imaging in predicting the response of osteosarcoma to chemotherapy. *Invest. Radiol. 27*, 847-855 (1992).

26. Hawighorst, H., Essig, M., Debus, J., Knopp, M. V., Engenhart-Cabilic, R., Schonberg, S. O., Brix, G., Zuna, I., van Kaick, G. Serial MR imaging of intracranial metastases after radiosurgery. *Magn. Reson. Imaging 15*, 1121-1132 (1997).

27. Hawighorst, H., Engenhart, R., Knopp, M. V., Brix, G., Grandy, M., Essig, M., Miltner, P., Zuna, I., Fuss, M., van Kaick, G. Intracranial meningeomas: Time- and dose-dependent effects of irradiation on tumor microcirculation monitored by dynamic MR imaging. *Magn. Reson. Imaging 15*, 423-432 (1997).